Alessandro VENEZIANI
Department of Math&CS
Emory University

Data Driven Computations in the Life Sciences
Autumn School and Workshop,
November 9-13, 2015, IST, Lisbon

Geometrical Multiscale Models for the Cardiovascular System - II

Defective Boundary Data Problems (I)

Coupling of Dimensionally Heterogeneous Models

Outline

1 . A **different approach for defective conditions**
(in the “data assimilation” direction)

2. The **Geometrical Multiscale** Framework
   2.1 Basic principles
   2.2 Examples
   - A simple 1D/0D model
   - An academic 3D/0D case
   - A real 3D/0D case

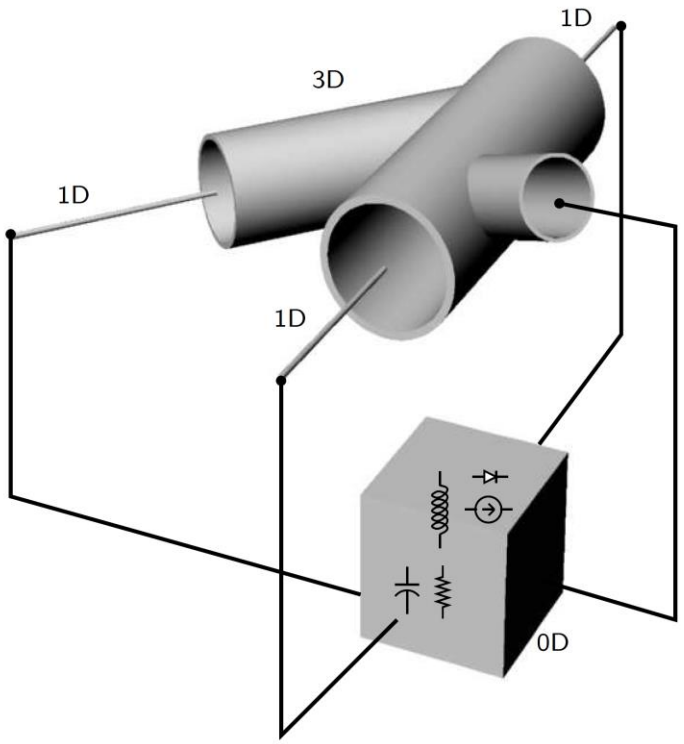

Main References

1. L. Formaggia, A. Quarteroni, A. Veneziani, Multiscale modelling of the Vascular System, Chapter 11 in “Cardiovascular Mathematics”, L. Formaggia, A. Quarteroni, A. Veneziani (eds.), Springer 2009
2. A. Quarteroni, A. Veneziani, C. Vergara, “Geometrical Multiscale Modeling of the Circulatory System, between Theory and Practice”, Tech Report available at www.mathcs.emory.edu, 2015

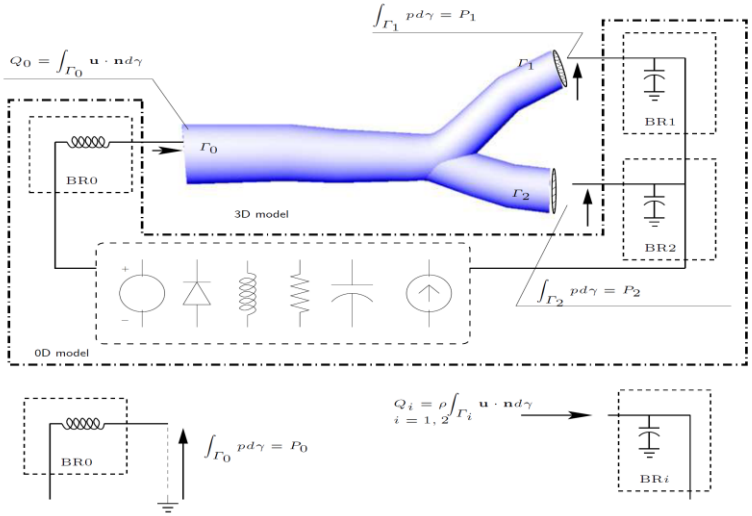

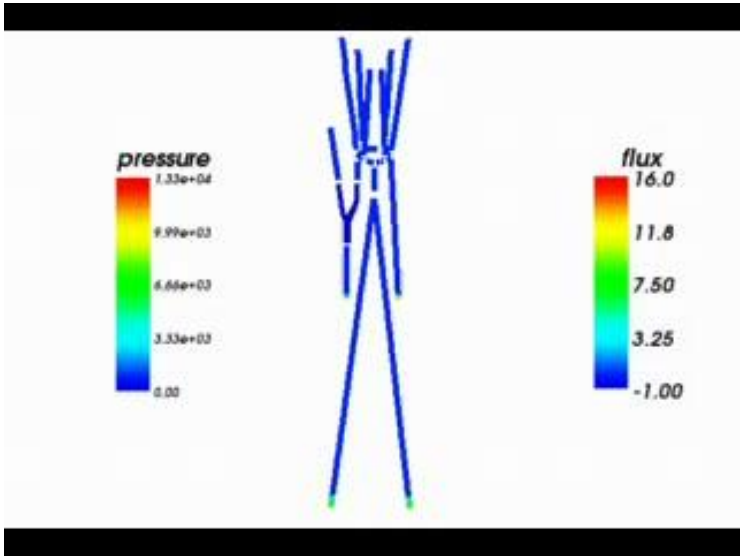

A twist in the tale: the "control" approach

Basic ideas

In the augmented formulation:

- The Navier-Stokes equations play the role of **state equations**
- The flow rate conditions are constraints for the solution

Let us swap the roles:

1. We introduce **an appropriate functional J related to the conditions to be minimized**
2. The **Navier-Stokes equations as constraints** to the minimization process

Minimization will be pursued by acting on **(control) boundary values**

The flow rate problem

For the sake of simplicity, we refer to the **steady Stokes problem.**

Let us introduce the functional:

$$\mathcal{J}(\mathbf{w}) \equiv \sum_{i=1}^{m} \frac{1}{2} \left(\int_{\Gamma_i} \mathbf{w} \cdot \mathbf{n} d\gamma - F_i \right)^2$$

We look for the solution minimizing this functional with the ***constraint given by the Stokes equations:***

$$\begin{cases} -\mu \triangle \boldsymbol{u}(\boldsymbol{k}) + \nabla p(\boldsymbol{k}) = \boldsymbol{f}, & \boldsymbol{x} \in \Omega \\ \nabla \cdot \boldsymbol{u}(\boldsymbol{k}) = 0, & \boldsymbol{x} \in \Omega \\ \boldsymbol{u}(\boldsymbol{k})|_{\Gamma_w} = \mathbf{0} \\ (-p(\boldsymbol{k})\boldsymbol{n} + \mu \nabla \boldsymbol{u}(\boldsymbol{k})\, \boldsymbol{n})|_{\Gamma_0} = \mathbf{0}, \\ (-p(\boldsymbol{k})\boldsymbol{n} + \mu \nabla \boldsymbol{u}(\boldsymbol{k})\, \boldsymbol{n})|_{\Gamma_i} = -k_i \boldsymbol{n}, & i = 1, \ldots, m, \end{cases}$$

We put in evidence the role of the ***"control" variables:***

$$\boldsymbol{k} = (k_1, \ldots, k_m) \in \mathbb{R}^m$$

The constrained functional reads:

$$\mathcal{L}(\boldsymbol{w}, s; \boldsymbol{\lambda}_w, \lambda_s; \boldsymbol{\eta}) = \quad \mathcal{J}(\boldsymbol{w}) + \mu(\nabla \boldsymbol{w}, \nabla \boldsymbol{\lambda}_w) + \\ -(s, \nabla \cdot \boldsymbol{\lambda}_w) + \sum_{i=1}^{m} \int_{\Gamma_i} \eta_i \boldsymbol{\lambda}_w \cdot \boldsymbol{n} \, d\gamma - (\boldsymbol{f}, \boldsymbol{\lambda}_w) - (\lambda_s, \nabla \cdot \boldsymbol{w}).$$

Searching for **stationary points of this functional**, we have the **KKT** problem:

$$\begin{cases} (P) \begin{cases} < d\mathcal{L}_{\boldsymbol{\lambda}_w}, \boldsymbol{v} >= \mu(\nabla \boldsymbol{u}, \nabla \boldsymbol{v}) - (p, \nabla \cdot \boldsymbol{v}) + \sum_{i=1}^{m} \int_{\Gamma_i} k_i \boldsymbol{v} \cdot \boldsymbol{n} \, d\gamma - (\boldsymbol{f}, \boldsymbol{v}) = 0, \\ < d\mathcal{L}_{\lambda_s}, q >= -(q, \nabla \cdot \boldsymbol{u}) = 0, \end{cases} \\ (A) \begin{cases} < d\mathcal{L}_{\boldsymbol{w}}, \boldsymbol{v} >= \mu(\nabla \boldsymbol{v}, \nabla \boldsymbol{\lambda}_u) - (\lambda_p, \nabla \cdot \boldsymbol{v}) - \sum_{i=1}^{m} \left(\int_{\Gamma_i} \boldsymbol{u} \cdot \boldsymbol{n} \, d\gamma - F_i \right) \int_{\Gamma_i} \boldsymbol{v} \cdot \boldsymbol{n} \, d\gamma = 0, \\ < d\mathcal{L}_s, q >= -(q, \nabla \cdot \boldsymbol{\lambda}_u) = 0, \end{cases} \\ (C_j) \quad < d\mathcal{L}_{\eta_j}, \nu >= \int_{\Gamma_j} \nu \boldsymbol{\lambda}_u \cdot \boldsymbol{n} \, d\gamma = 0, \quad j = 1, \ldots, m. \end{cases}$$

Stokes problem

Adjoint problem

Optimality conditions

Observe that ***the adjoint problem is still a Stokes-like system:***

$$
\begin{cases}
-\mu\triangle\boldsymbol{\lambda}_u + \nabla\lambda_p = \mathbf{0}, & \boldsymbol{x}\in\Omega,\\
\nabla\cdot\boldsymbol{\lambda}_u = 0, & \boldsymbol{x}\in\Omega,\\
\boldsymbol{\lambda}_u|_{\Gamma_w} = \mathbf{0},\\
(-\lambda_p\boldsymbol{n} + \mu\nabla\boldsymbol{\lambda}_u\ \boldsymbol{n})|_{\Gamma_0} = \mathbf{0},\\
(-\lambda_p\boldsymbol{n} + \mu\nabla\boldsymbol{\lambda}_u\ \boldsymbol{n})|_{\Gamma_i} = \Big(\displaystyle\int_{\Gamma_i}\boldsymbol{u}\cdot\boldsymbol{n}\,d\gamma - F_i\Big)\boldsymbol{n}, & i=1,\dots,m.
\end{cases}
$$

Remarks

1. The formulation can be extended to the **unsteady NS system**:
   a) Fixed point strategy for the non-linearity
   b) Application to the time discretized problem (some concerns, see later)
2. **Well posedness analysis** of the constrained minimization problem can be carried out by means of a fixed-point strategy

Numerical solution of the control problem

At the numerical level, *an iterative procedure is needed for solving the problem*, with the successive solution of (*P*)-(*A*) and (C_j) acting as convergence conditions

$$\mathbf{k}^n \mapsto \text{Solve (P)}$$
$$\hookrightarrow (\boldsymbol{u}, p) \mapsto \text{Solve (A)}$$
$$\hookrightarrow (\lambda_{\boldsymbol{u}}, \lambda_p) \mapsto \text{fulfillment of (C)}$$

$$\text{if } \int_\Gamma \lambda_{\boldsymbol{u}} \cdot \boldsymbol{n} d\gamma \neq 0 \text{ then } \mathbf{k}^{n+1} = \mathbf{k}^n + \tau^n \int_\Gamma \lambda_{\boldsymbol{u}}^n \cdot \boldsymbol{n} d\gamma$$

τ is a relaxation parameter (< 0)

THEOREM: For a proper choice of τ, this algorithm converges to the solution

Selection of the relaxation parameter

Steepest descent strategy:

$$\tau^l = \tau_N^l = -\frac{J_Q(\boldsymbol{u}_h^l)}{\|\mathcal{L}_{\boldsymbol{k}}(\boldsymbol{s}_h^l)\|_2^2}$$

It is possible to verify that this corresponds to apply the Newton method to the equation $J_Q(\boldsymbol{u}^l{}_h(\boldsymbol{k}^l))=0$.

Since J_Q is a quadratic functional, we guess: $\tau = 2\tau^l{}_N$

	τ =-1	$\tau = \tau^n{}_N$	$\tau = \tau^n{}_N$ + AITKEN	$\tau = 2\tau^n{}_N$	LM
Steady	87	22	4	2	2
Unsteady	-	5.08	3.81	1.98	2

Remarks (cont'd)

3. Numerical results are comparable with the ones of the LM approach.
4. This **approach is however more versatile**

Numerical Results

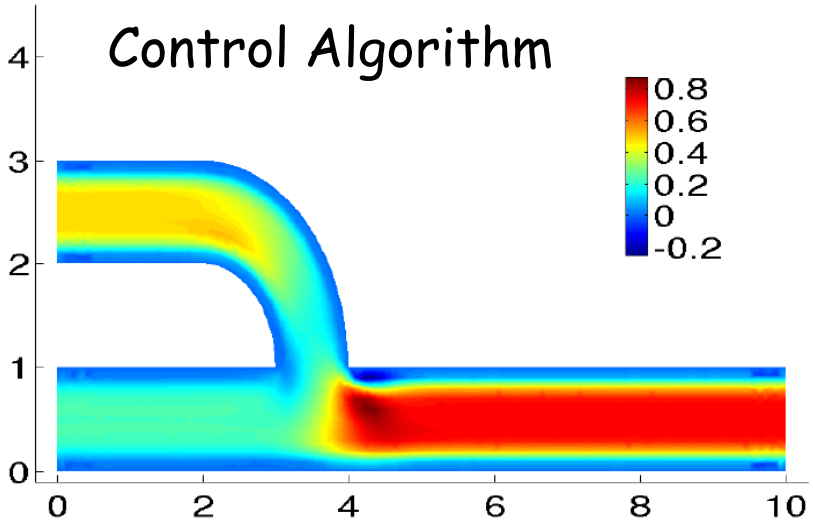

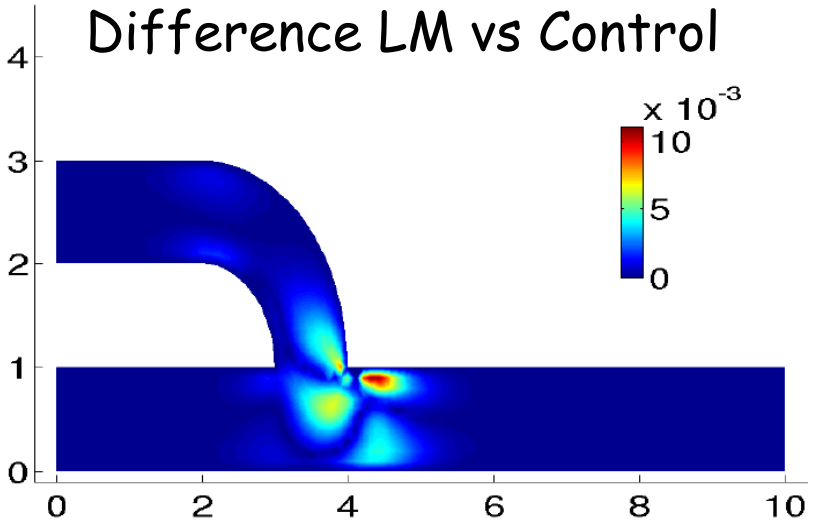

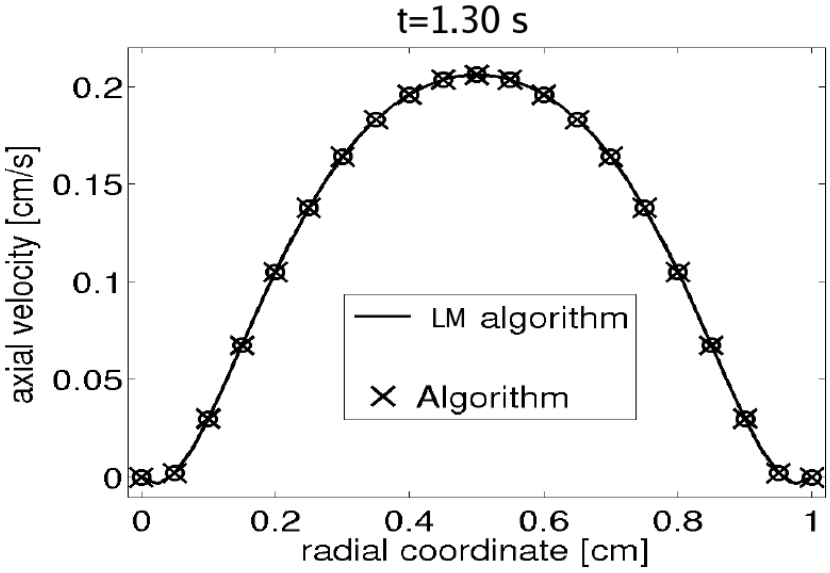

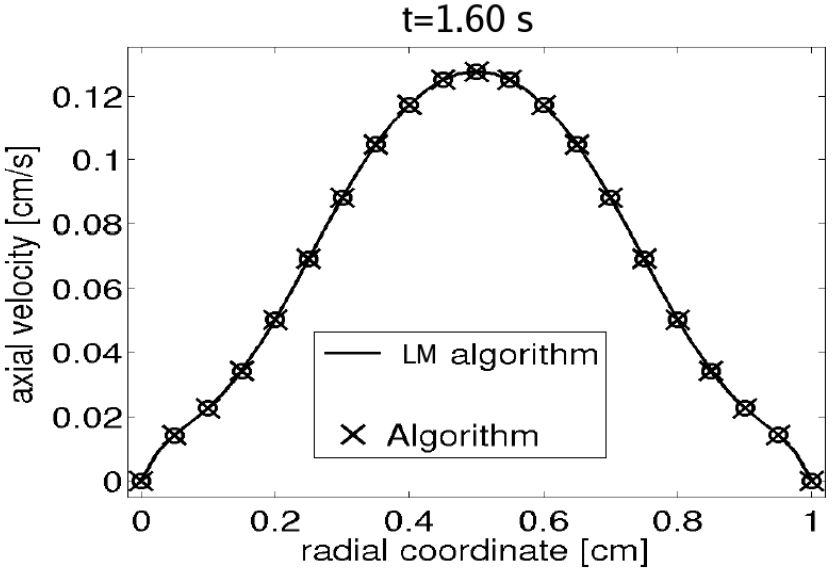

The mean pressure drop problem

Functional:

$$J_P(s) = \frac{1}{2}\Big(\sum_{i=0}^{m} \frac{1}{|\Gamma_i|}\int_{\Gamma_i} s\, d\gamma - P_i\Big)^2.$$

Constraints:

$$\begin{cases} -\mu\triangle \boldsymbol{u}(\boldsymbol{Q}) + \nabla p(\boldsymbol{Q}) = \boldsymbol{f}, & \boldsymbol{x}\in\Omega, \\ \nabla\cdot\boldsymbol{u}(\boldsymbol{Q}) = 0 & \boldsymbol{x}\in\Omega, \\ \boldsymbol{u}(\boldsymbol{Q})|_{\Gamma_w} = \boldsymbol{0}, & \\ (-p(\boldsymbol{Q})\boldsymbol{n} + \mu\nabla\boldsymbol{u}(\boldsymbol{Q})\,\boldsymbol{n})|_{\Gamma_0} = -P_0\boldsymbol{n}, & \\ \displaystyle\int_{\Gamma_j} \boldsymbol{u}(\boldsymbol{Q})\cdot\boldsymbol{n}\, d\gamma = Q_j, & j = 1,\ldots,m. \end{cases}$$

Constrained functional:

$$\begin{aligned}\mathcal{L}(\boldsymbol{w}, s, \boldsymbol{\xi}; \boldsymbol{\lambda}_w, \lambda_s, \boldsymbol{\lambda}_\xi; \boldsymbol{\eta}) = \quad & J_P(s) + \mu(\nabla\boldsymbol{w}, \nabla\boldsymbol{\lambda}_w) - (s, \nabla\cdot\boldsymbol{\lambda}_w) + \sum_{i=1}^{m}\xi_i\int_{\Gamma_i}\boldsymbol{\lambda}_w\cdot\boldsymbol{n}\, d\gamma + \\ & -(\boldsymbol{f}, \boldsymbol{\lambda}_w) - (\lambda_s, \nabla\cdot\boldsymbol{w}) + \sum_{i=1}^{m}\lambda_{\xi_i}\Big(\int_{\Gamma_i}\boldsymbol{w}\cdot\boldsymbol{n}\, d\gamma - \eta_i\Big).\end{aligned}$$

Given $\boldsymbol{f} \in \boldsymbol{L}^2(\Omega)$ and $P_j \in \mathbb{R}$, $j = 1, \ldots, m$, find $\boldsymbol{u} = \boldsymbol{u}(\boldsymbol{Q}) \in \boldsymbol{V}, p(\boldsymbol{Q}) \in H^1(\Omega), \zeta_j(\boldsymbol{Q}) \in \mathbb{R}$, $j = 1, \ldots, m$, $\boldsymbol{\lambda}_u \in \boldsymbol{V}, \lambda_p \in L^2(\Omega), \lambda_{\zeta_j} \in \mathbb{R}$, $j = 1, \ldots, m$, and $\boldsymbol{Q} \in \mathbb{R}^m$ such that, for all $\boldsymbol{v} \in \boldsymbol{V}$, $q \in L^2(\Omega)$ and $\nu \in \mathbb{R}$:

$$
\begin{cases}
(P) \begin{cases}
< d\mathcal{L}_{\boldsymbol{\lambda}_u}, \boldsymbol{v} >= \mu(\nabla \boldsymbol{u}, \nabla \boldsymbol{v}) - (p, \nabla \cdot \boldsymbol{v}) + \displaystyle\sum_{i=1}^{m} \zeta_i \int_{\Gamma_i} \boldsymbol{v} \cdot \boldsymbol{n}\, d\gamma - (\boldsymbol{f}, \boldsymbol{v}) = 0, \\
< d\mathcal{L}_{\lambda_p}, q >= -(q, \nabla \cdot \boldsymbol{u}) = 0, \\
< d\mathcal{L}_{\lambda_{\zeta_i}}, \nu >= \Big(\displaystyle\int_{\Gamma_i} \boldsymbol{u} \cdot \boldsymbol{n}\, d\gamma - Q_i \Big) \nu = 0,
\end{cases} \\
(A) \begin{cases}
< d\mathcal{L}_{\boldsymbol{u}}, \boldsymbol{v} >= \mu(\nabla \boldsymbol{v}, \nabla \boldsymbol{\lambda}_u) - (\lambda_p, \nabla \cdot \boldsymbol{v}) + \displaystyle\sum_{i=1}^{m} \lambda_{\zeta_i} \int_{\Gamma_i} \boldsymbol{v} \cdot \boldsymbol{n}\, d\gamma = 0, \\
< d\mathcal{L}_p, q >= \displaystyle\sum_{i=1}^{m} \Big(\frac{1}{|\Gamma_i|} \int_{\Gamma_i} p\, d\gamma - P_i \Big) \frac{1}{|\Gamma_i|} \int_{\Gamma_i} q\, d\gamma - (q, \nabla \cdot \boldsymbol{\lambda}_u) = 0, \\
< d\mathcal{L}_{\zeta_i}, \nu >= \Big(\displaystyle\int_{\Gamma_i} \boldsymbol{\lambda}_u \cdot \boldsymbol{n}\, d\gamma \Big) \nu = 0,
\end{cases} \\
(C_i) \quad < d\mathcal{L}_{Q_i}, \nu >= -\lambda_{\zeta_i} \nu = 0, \quad i = 1, \ldots, m
\end{cases}
$$

REMARKS:

1. Different formulations can be devised with different control variables sets (e.g. the ***normal stresses***)
2. The functional can be devised in order to incorporate informations on the solution (***versatility***)

Not necessarily we have data on the boundary in practice…

Yet with this approach we can “assimilate” these data

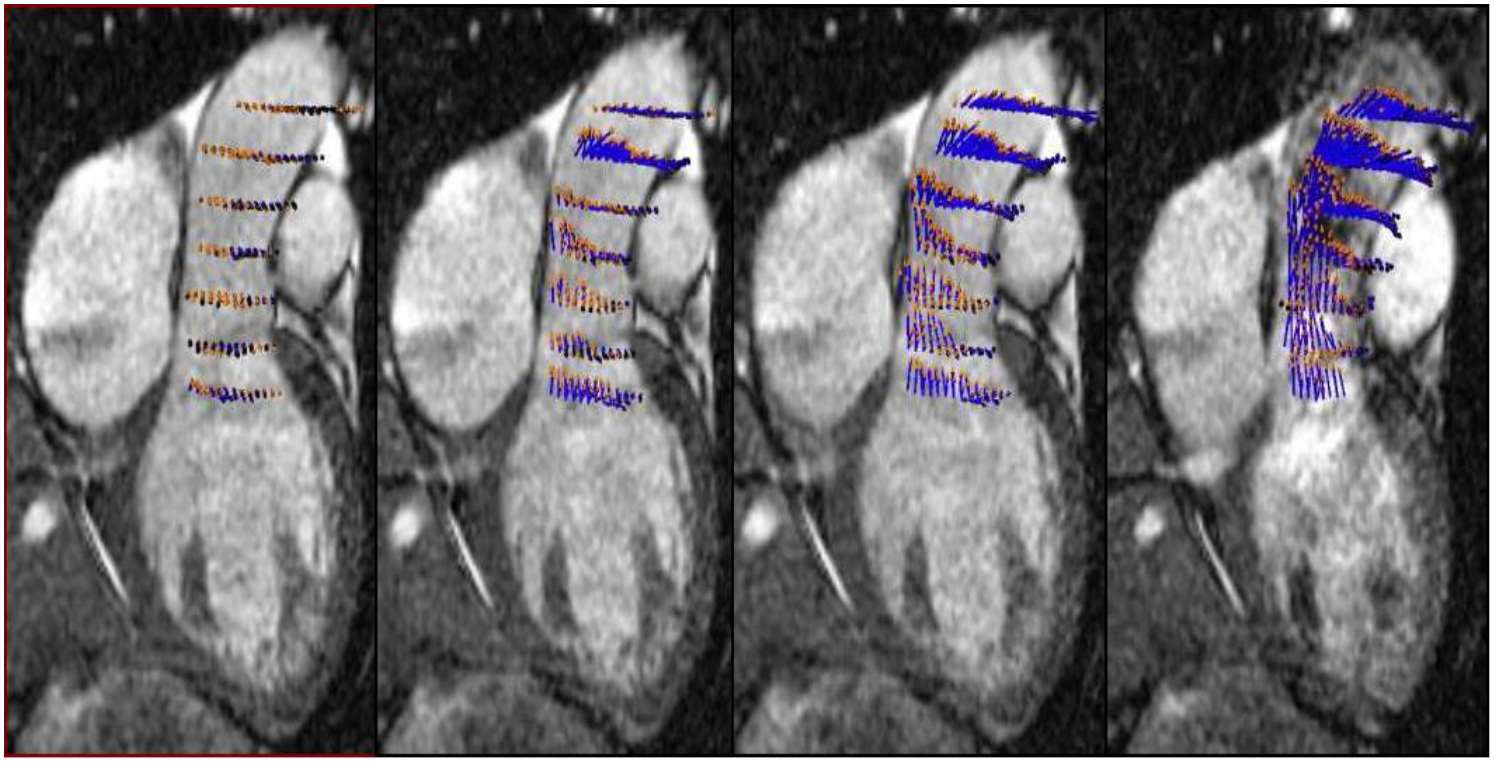

See M. D’Elia, Perego, Veneziani JSC and D’Elia, Veneziani M2AN

Numerical results

1) Womersley test case

Comparison for formulations with ***different control variables***

L^2-*errors*

Time	Flow rate as control variables	Normal stress control variables
$t = 1.10\ s$	$9.327 \cdot 10^{-5}$	$9.329 \cdot 10^{-5}$
$t = 1.40\ s$	$3.569 \cdot 10^{-5}$	$3.578 \cdot 10^{-5}$

Pressure profile

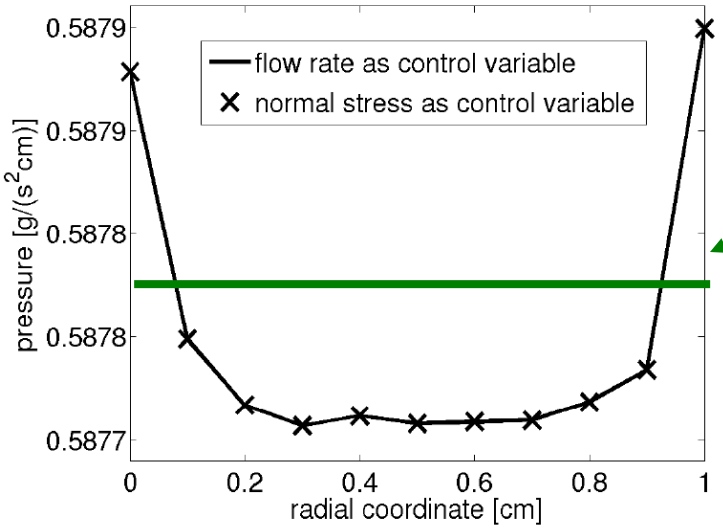

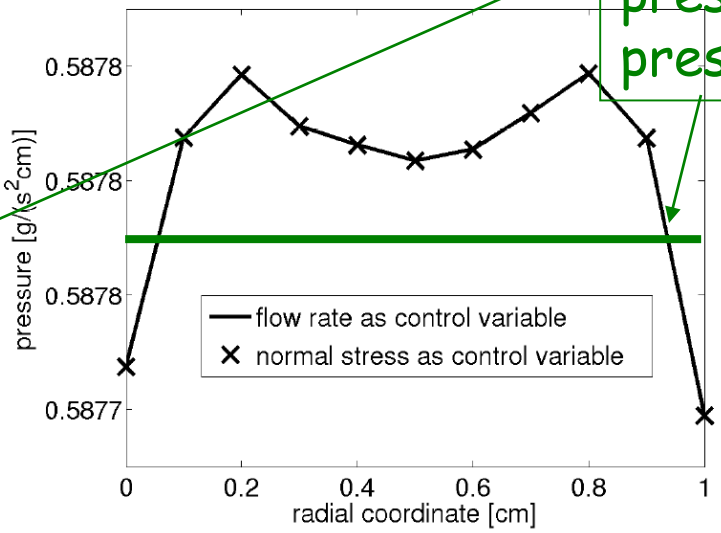

Mean pressure prescribed

What about the structure?

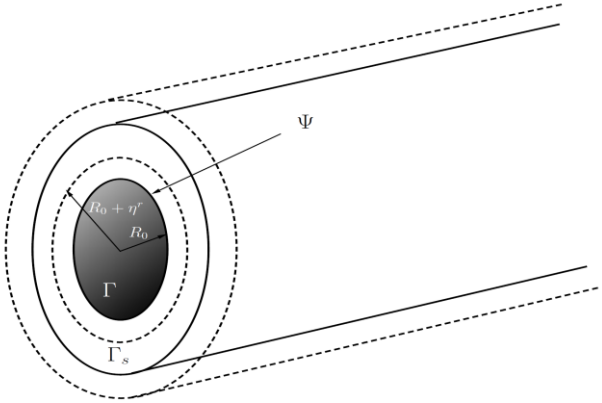

For the sake of brevity we do not address structure coupling in detail
Let us consider briefly **"defective" conditions for the structure**

The problem is not largely considered – "practical" solutions

Example: if we have the area, this can be regarded as an average of the radial displacement

$$A = \int_0^{\eta} da$$

As for the average velocity, we can assume a "profile" (e.g. circular) that fits this relation (Dirichlet conditions).
In principle, we can also use a Lagrange multiplier approach.

Conditions on the normal stresses are usually set to zero
(see A. Quarteroni, A.V., C. Vergara 2015 and references for details)

Some results on the compliant case

Situation is much *more complicated* by the presence of *different iterative processes*:

1. Time advancing
2. Fluid-Structure interaction algorithms
3. Solution of the (Partitioned) Augmented Defective Problem or the Control Problem

High Computational Costs!!!

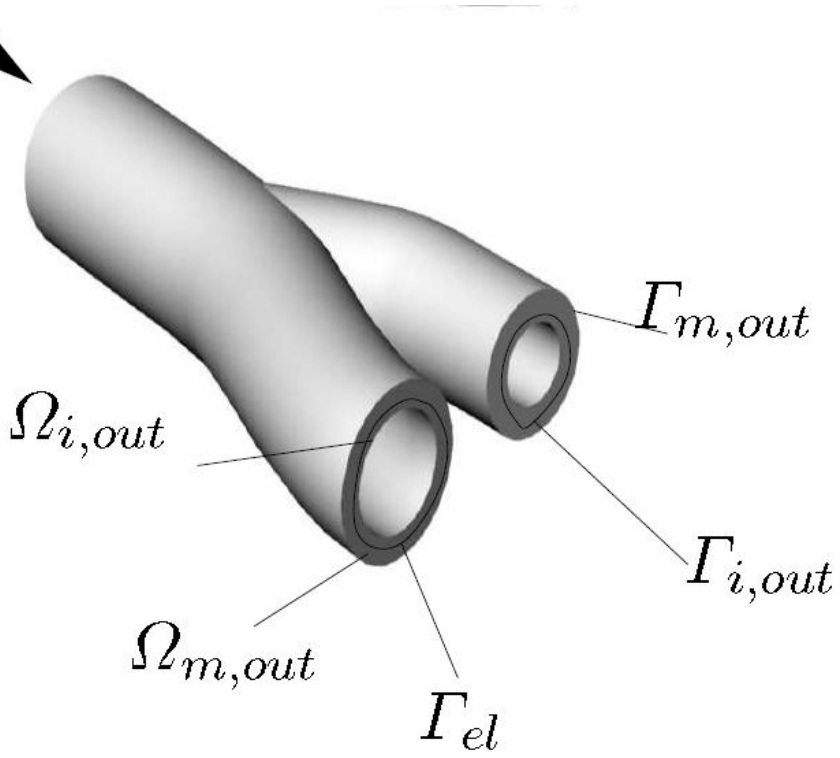

C. Vergara, A. Veneziani, L. Formaggia 2009

An example based on the “control” approach

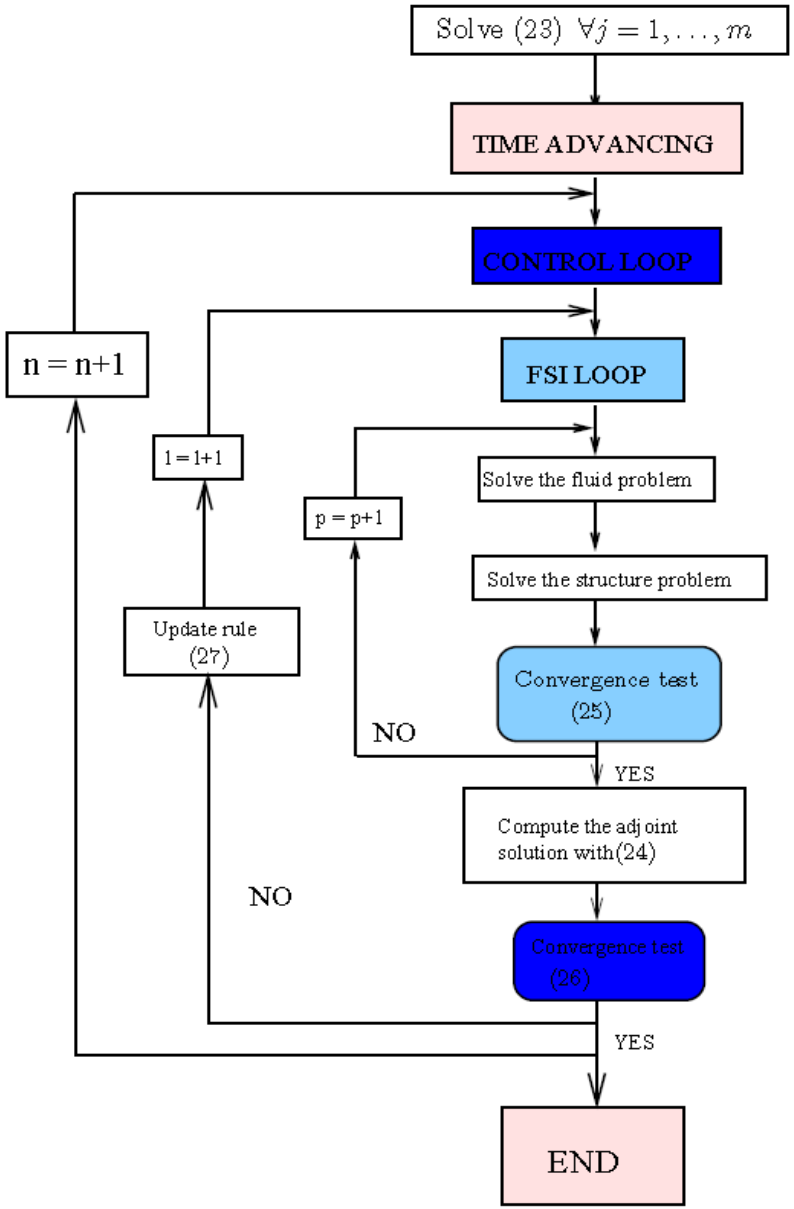

…and a possible simplification:

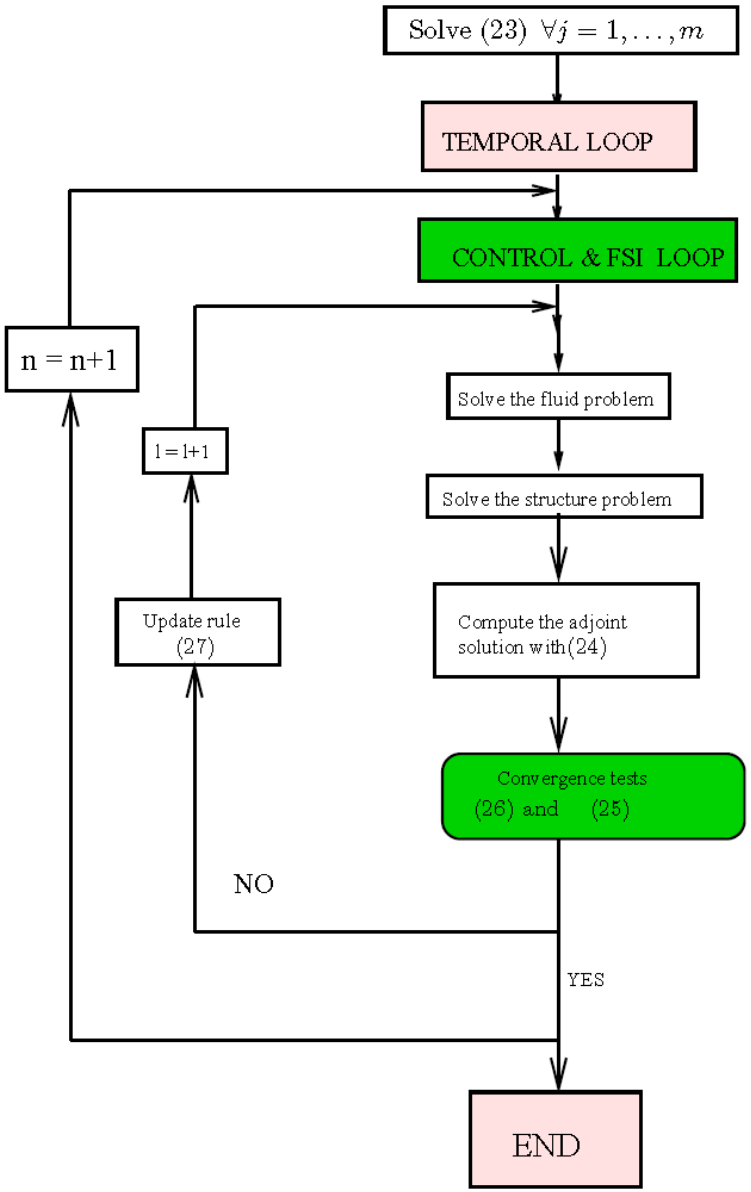

Pressure in a simplified 2D carotid bifurcation

Pressure

Pressure difference of the 2 algorithms

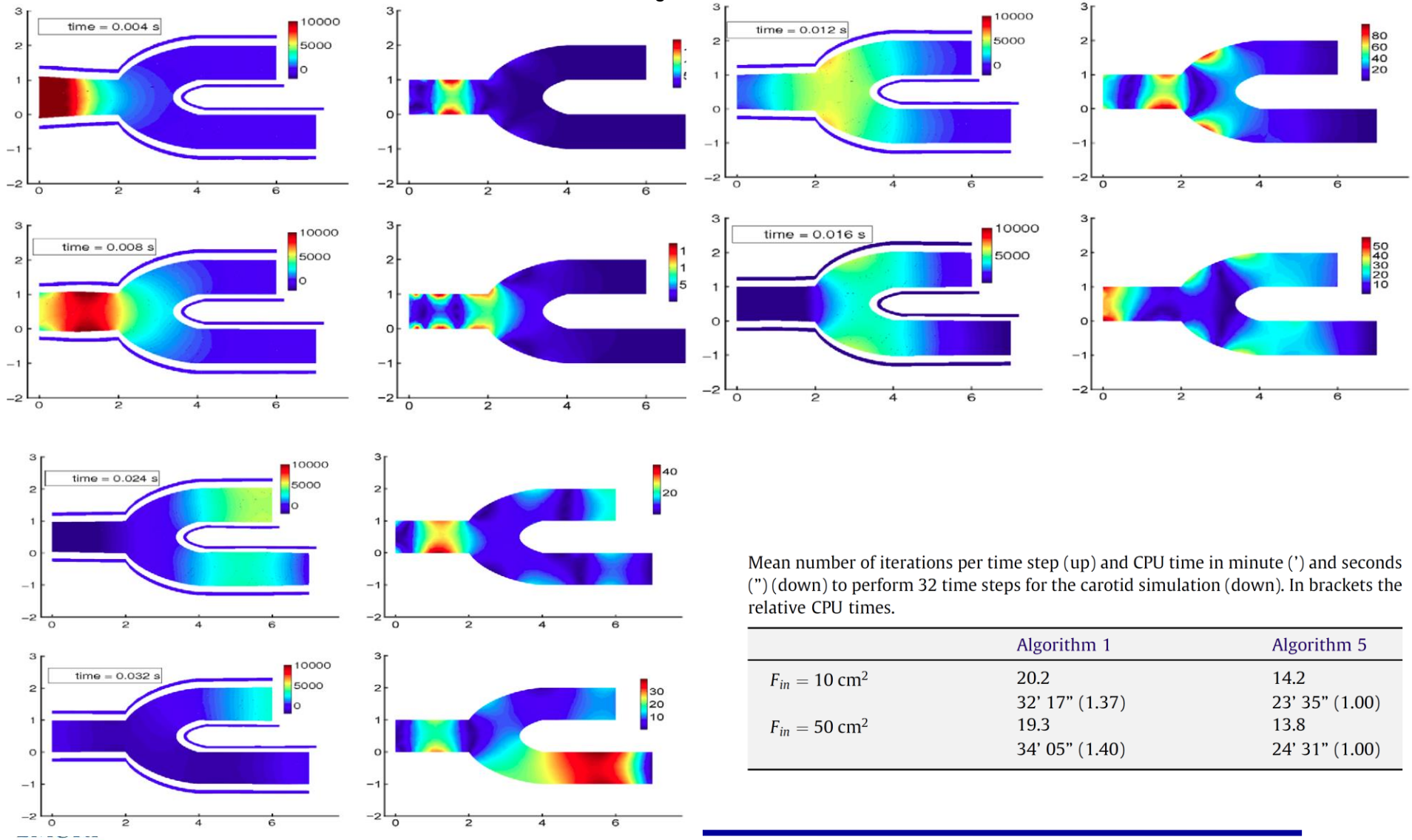

Mean number of iterations per time step (up) and CPU time in minute (') and seconds (") (down) to perform 32 time steps for the carotid simulation (down). In brackets the relative CPU times.

	Algorithm 1	Algorithm 5
$F_{in} = 10$ cm^2	20.2	14.2
	32' 17" (1.37)	23' 35" (1.00)
$F_{in} = 50$ cm^2	19.3	13.8
	34' 05" (1.40)	24' 31" (1.00)

The mean pressure drop problem

Functional:

$$J_P(s) = \frac{1}{2}\Big(\sum_{i=0}^{m} \frac{1}{|\Gamma_i|}\int_{\Gamma_i} s\, d\gamma - P_i\Big)^2.$$

Constraints:

$$\begin{cases} -\mu\Delta \boldsymbol{u}(\boldsymbol{k}) + \nabla p(\boldsymbol{k}) = \boldsymbol{f} & \text{in } \Omega, \\ \nabla \cdot \boldsymbol{u}(\boldsymbol{k}) = 0 & \text{in } \Omega, \\ \boldsymbol{u}|_{\Gamma_w} = \boldsymbol{0}, & \\ -p(\boldsymbol{k})\boldsymbol{n} + \mu\nabla \boldsymbol{u}(\boldsymbol{k})\cdot \boldsymbol{n}|_{\Gamma_i} = -k_i\boldsymbol{n} & \text{on } \Gamma_i, i = 0, 2, \ldots, m \end{cases}$$

Constrained functional:

$$\mathcal{L}(\boldsymbol{w}, s; \boldsymbol{\lambda}_w, \lambda_s; \boldsymbol{\eta}) = J_P(s) + a(\boldsymbol{w}, \boldsymbol{\lambda}_w) - (s, \nabla\cdot\boldsymbol{\lambda}_w) +$$

$$\sum_{i=0}^{m}\int_{\Gamma_i} \eta_i \boldsymbol{\lambda}_w\cdot\boldsymbol{n}\, d\gamma - (\boldsymbol{f}, \boldsymbol{\lambda}_w) - (\lambda_s, \nabla\cdot\boldsymbol{w})$$

Given $\boldsymbol{f} \in \boldsymbol{L}^2(\Omega)$ *and* $\boldsymbol{P} \in \mathbb{R}^{m+1}$, *find* $\boldsymbol{k} \in \mathbb{R}^{m+1}$, $\boldsymbol{u}(\boldsymbol{k}) \in \boldsymbol{V}, p(\boldsymbol{k}) \in H^1(\Omega), \boldsymbol{\lambda}_u \in \boldsymbol{V}$ *and* $\lambda_p \in H^1(\Omega)$, *such that, for all* $\boldsymbol{v} \in \boldsymbol{V}$, $q \in H^1(\Omega)$ *and* $\nu \in \mathbb{R}$,

$$
\begin{cases}
(P) \begin{cases} < d\mathcal{L}_{\boldsymbol{\lambda}_u}, \boldsymbol{v} >= (\nabla \boldsymbol{u}, \nabla \boldsymbol{v}) - (p, \nabla \cdot \boldsymbol{v}) + \displaystyle\sum_{i=0}^{m} \int_{\Gamma_i} k_i \boldsymbol{v} \cdot \boldsymbol{n} \, d\gamma - (\boldsymbol{f}, \boldsymbol{v}) = 0, \\ < d\mathcal{L}_{\lambda_p}, q >= -(q, \nabla \cdot \boldsymbol{u}) = 0, \end{cases} \\
(A) \begin{cases} < d\mathcal{L}_{\boldsymbol{u}}, \boldsymbol{v} >= (\nabla \boldsymbol{v}, \nabla \boldsymbol{\lambda}_u) - (\lambda_p, \nabla \cdot \boldsymbol{v}) = 0, \\ < d\mathcal{L}_p, q >= \displaystyle\sum_{i=0}^{m} \Big(\frac{1}{|\Gamma_i|} \int_{\Gamma_i} p \, d\gamma - P_i \Big) \frac{1}{|\Gamma_i|} \int_{\Gamma_i} q \, d\gamma - (q, \nabla \cdot \boldsymbol{\lambda}_u) = 0, \end{cases} \\
(C_j) \quad < d\mathcal{L}_{k_i}, \nu >= \displaystyle\int_{\Gamma_i} \nu \boldsymbol{\lambda}_u \cdot \boldsymbol{n} \, d\gamma = 0, \quad i = 0, \ldots, m.
\end{cases}
$$

REMARKS:

1. Different formulations can be devised with different control variables sets (e.g. the ***flow rates***)
2. Well posedness analysis is **missing** (!)
3. The functional can be devised in order to incorporate informations on the solution (***versatility***)
4. A fixed point numerical algorithm can still be devised: however, theoretical convergence analysis is **missing**. It is possible to prove that the *sequence of iterations does not diverge*. In numerical tests, it converges.

MULTISCALE FRAMEWORK

- Coupling schemes for 3D/1D/0D models
  - Interface Conditions
  - Coupling Algorithms

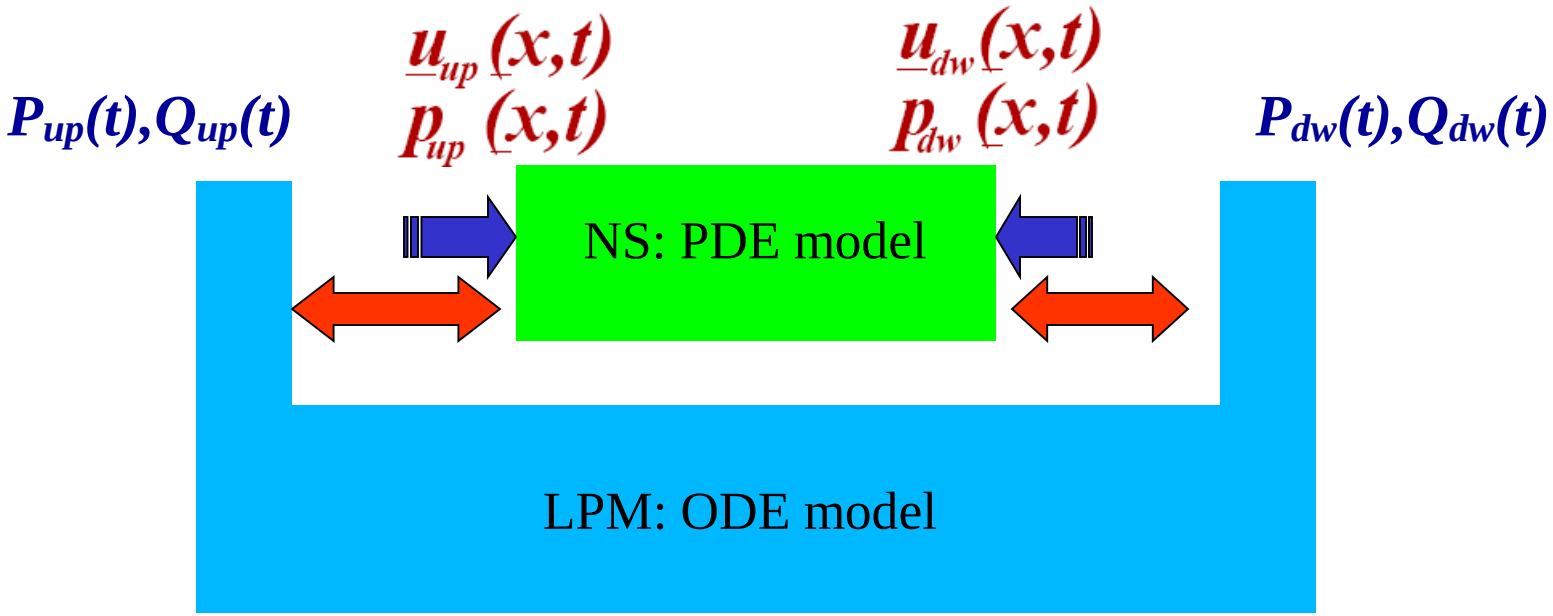

Numerical Coupling of Different Models

Coupling 3D/0D models

A MONOLITHIC APPROACH (SIMPLE NETWORKS)

Semi-analytic approach:
Use the method of integrating factor to solve symbolically the 0D model eventually reduced to a bc.

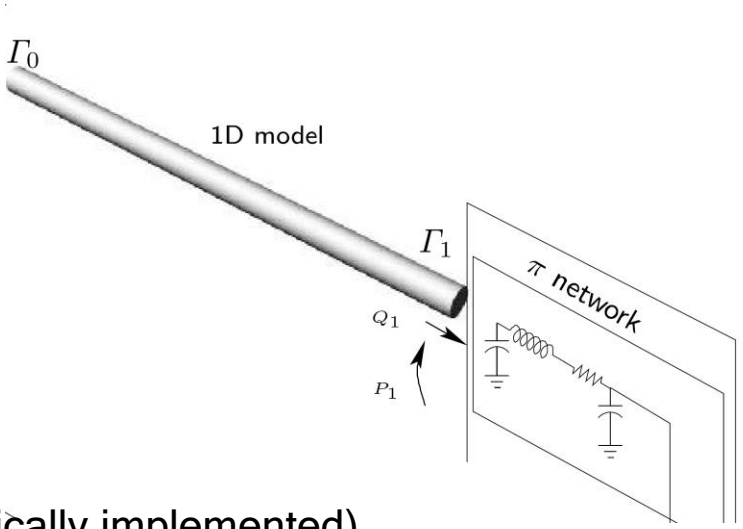

$$\frac{d(P_{0D} - R_1 Q_{0D})}{dt} + \frac{1}{R_2 C}(P_{0D} - R_1 Q_{0D}) = \frac{Q_{0D}}{C}$$

IF Method: Robin condition (to be properly numerically implemented)

$$P_{0D}(t) = R_1 Q_{0D}(t) + (P_{0D}(0) - R_1 Q_{0D}(0))\, e^{-t/(R_2 C)} + \frac{1}{C}\int_0^t e^{\tau - t/(R_2 C)} Q_{0D}(\tau) d\tau.$$

I. Vignon-Clementel, C. Taylor et al. (2006)

Numerical Coupling of Different Models

Coupling 3D/0D models

A DOMAIN DECOMPOSITION APPROACH

Multiscale = Domain splitting + Model Reduction

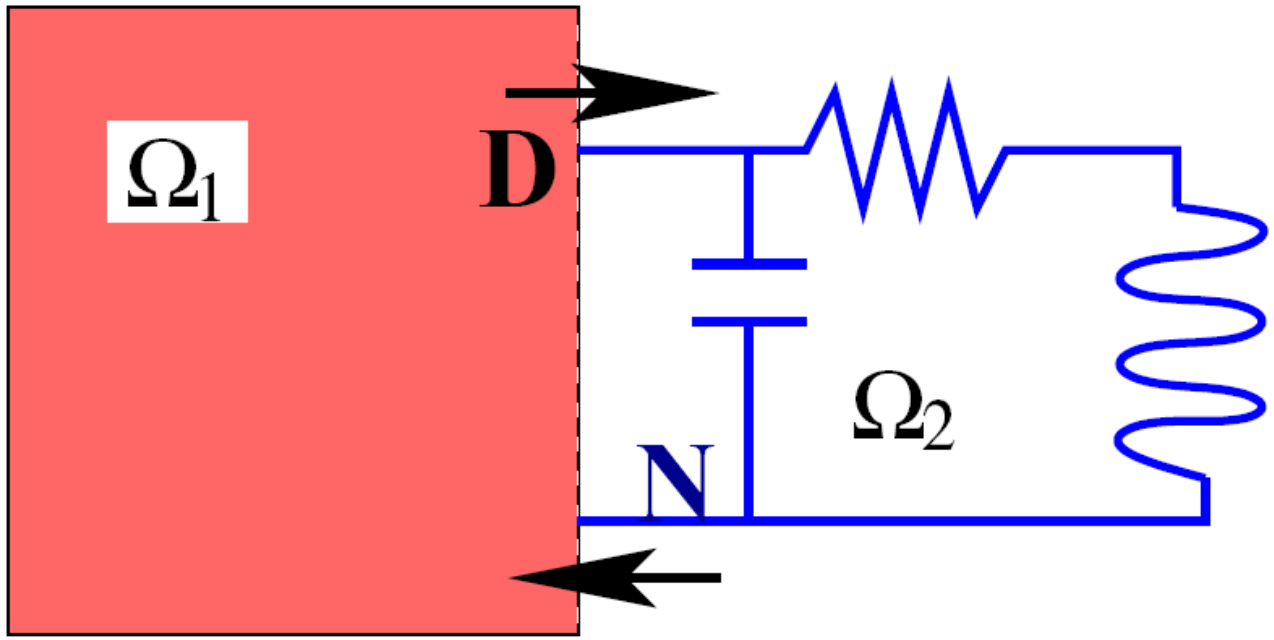

Bridging region compatibility

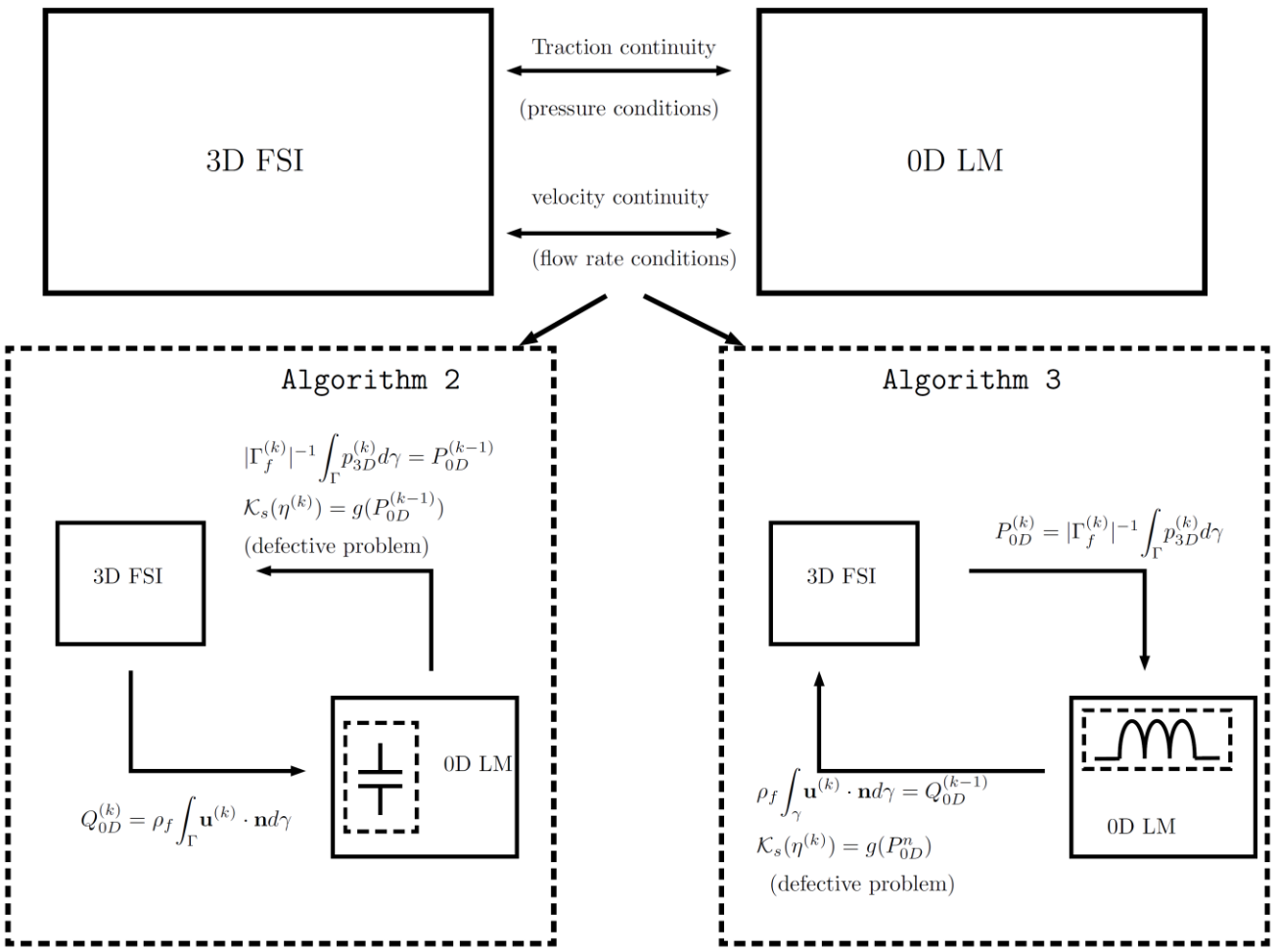

The 0D model incorporates the BC:

As for any nonoverlapping Domain Decomposition approach, **we are not free of selecting arbitrary interface conditions.**

With model reduction this **leads to some compatibility between the decoupling algorithm and the topology of the 0D model**.

If you don't do this: see Marsden et al, JCP 2013.

Examples of coupled 3D/0D problems

Pressure-type interface

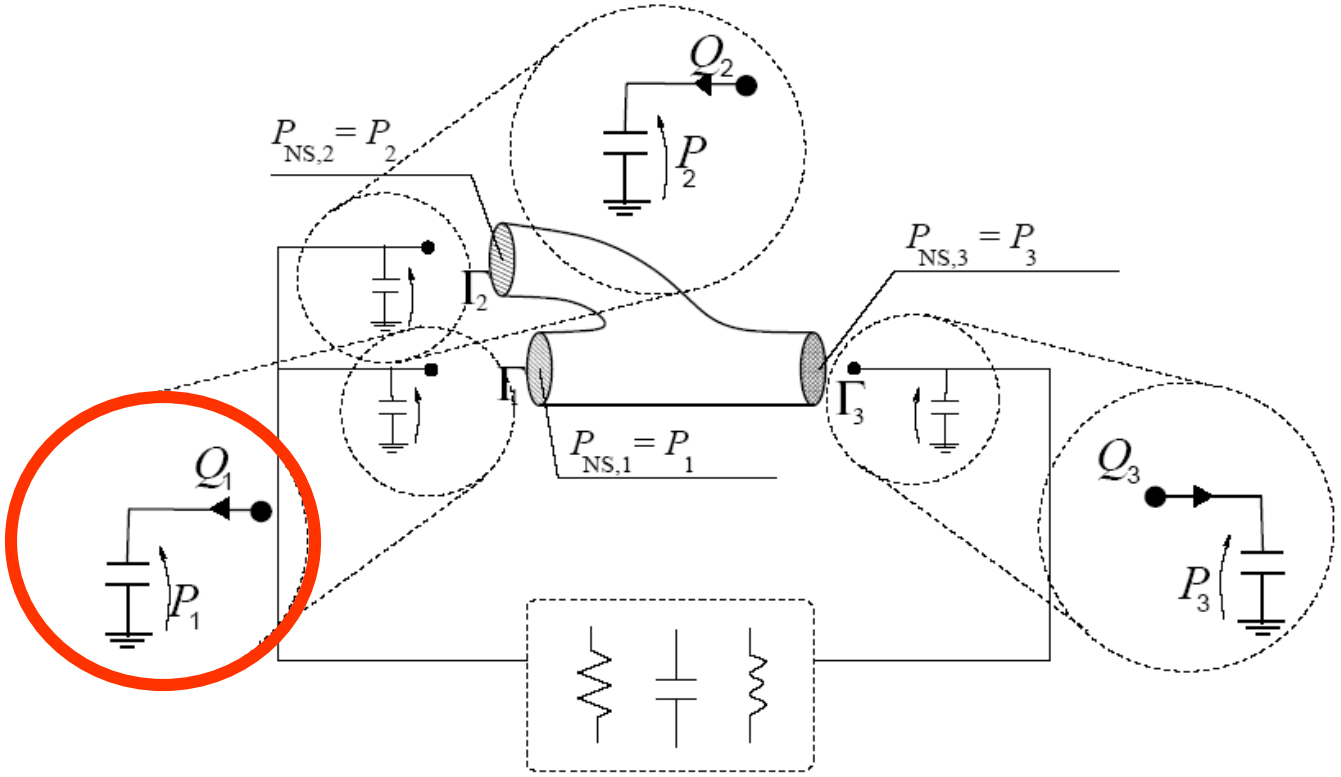

Examples of coupled 3D/0D problems

Flux-type interface

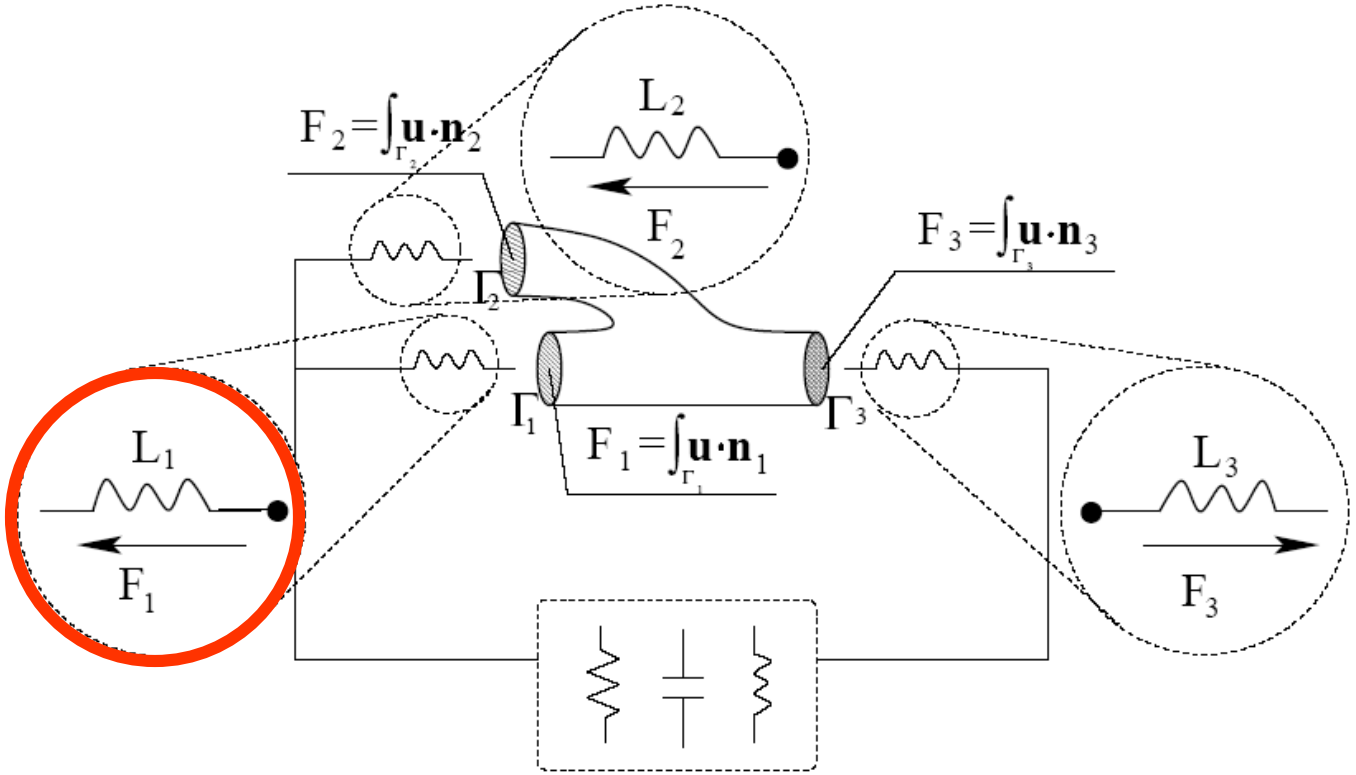

Well posedness analysis of heterogeneous models

Quarteroni, V., SIAM MMS, 2003

Refer to the Pressure-type interface problem

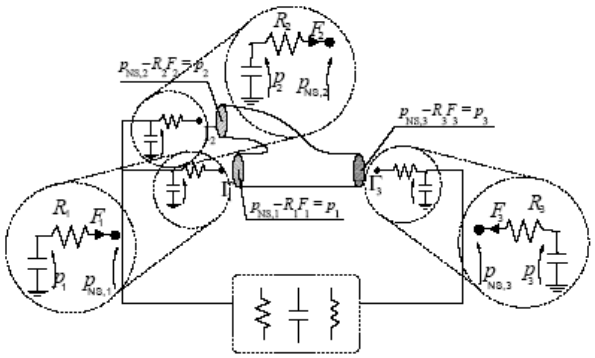

Given $\mathbf{u_0} \in \mathbf{V}^*$ e $\mathbf{y}_0 \in \mathbb{R}^m$, find $\mathbf{u} \in L^2(0,T;\mathbf{V})$ and $\mathbf{y} \in \mathbf{L}^\infty(0,T)$ s.t. $\forall t > 0$

$$\begin{cases} \dfrac{d\mathbf{y}}{dt} = A(\mathbf{y},t)\mathbf{y} + \mathbf{r}_H(\mathbf{y},t) + \mathbf{b}(\mathbf{F}(t)) \\ \left(\dfrac{\partial \mathbf{u}}{\partial t}, \boldsymbol{\varphi}\right) + a(\mathbf{u},\boldsymbol{\varphi}) + b(\mathbf{u},\mathbf{u},\boldsymbol{\varphi}) = c(\boldsymbol{\varphi}) \qquad \forall \boldsymbol{\varphi} \in \mathbf{V}^* \end{cases}$$

with $\mathbf{y}(0) = \mathbf{y}_0$, $\mathbf{u}|_{t=0} = \mathbf{u}_0$, and

$$\begin{cases} p_{NS,i}(t) = p_i(t) - R_i F_i(t) = y_i(t) - R_i F_i(t) \quad i = 1,\dots,\overline{n} \\ F_i(t) = \int_{\Gamma_i} \mathbf{u}\cdot\mathbf{n} d\boldsymbol{\gamma} \quad i = 1,\dots,\overline{n}. \end{cases}$$

"Complete" conditions: $p\mathbf{n} - \nu\nabla\mathbf{u}\cdot\mathbf{n} - K_i(\mathbf{u}\cdot\mathbf{n})\mathbf{n} = y_i\mathbf{n}$

Well Posedness Theorem

Suppose that initial data $\mathbf{y}_0$ and $\nabla \mathbf{u}_0$ are small enough. Then, assume:

$$\|A(\mathbf{z},t)\|_2 \leq C_A \quad \text{and} \quad |\mathbf{r}_H(\mathbf{z},t)| \leq C_H \qquad \forall \mathbf{z} \in \mathbf{L}^\infty(0,T), \forall t \in (0,T).$$

and $\kappa = \nu - 2Rc_2c_4 > 0$.

There exists a time $\tilde{T}$ $(0 < \tilde{T} \leq T)$ s.t. "multiscale" problem has at least one solution.

Sketch of the proof:

- ✓fixed point reformulation
- ✓sub-problems well posedness
- ✓compactness of the fixed-point operator (via Ascoli-Arzelà Theorem)
- ✓Schauder Theorem

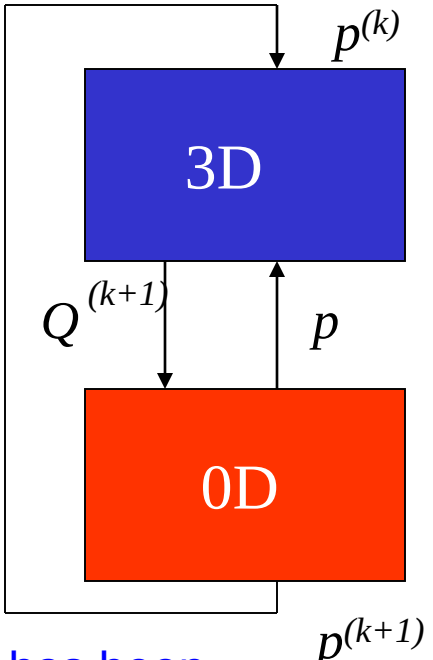

Remark: with a similar approach, a well posedness analysis has been carried out for 1D/0D models by Fernandez, Milisic (2004).

Coupling Algorithms

Time steps: $0 = t^0 < t^1 < \cdots < t^N = T$ with $\Delta t = t^{n+1} - t^n$ for $n = 0, \ldots, N-1$.

The Navier-Stokes system is solved by the finite element method for space variables and by a semi-implicit fractional step scheme for time advancement.

$N_{\mathbf{V}}$ and N_P are the number of velocity and pressure nodes.

$\mathbf{x} = [u_i, i = 1, \ldots, N_{\mathbf{V}}, p_j, j = 1, \ldots, N_{\mathbf{V}} + N_P]$ are the nodal values for the velocity and pressure.

The ODE system associated to the lumped model is solved by a finite difference scheme.

$$\begin{bmatrix} \mathcal{N}_1 & \mathcal{F}_{NET,1} \\ \mathcal{F}_{NS,1} & \mathcal{M}_1 \end{bmatrix} \begin{bmatrix} \mathbf{y}^{n+1} \\ \mathbf{x}^{n+1} \end{bmatrix} = \begin{bmatrix} \mathcal{N}_2 & \mathcal{F}_{NET,2} \\ \mathcal{F}_{NS,2} & \mathcal{M}_2 \end{bmatrix} \begin{bmatrix} \mathbf{y}^{n} \\ \mathbf{x}^{n} \end{bmatrix} + \begin{bmatrix} \mathbf{g} \\ \mathbf{0} \end{bmatrix}$$

$\mathcal{F}_{NS}$ and $\mathcal{F}_{NET,2}$ account for the treatment of the interface conditions.

The system may be solved by a Block Gauss-Siedel scheme $\Rightarrow$ staggered procedure.

Coupling Algorithms II: explicit schemes

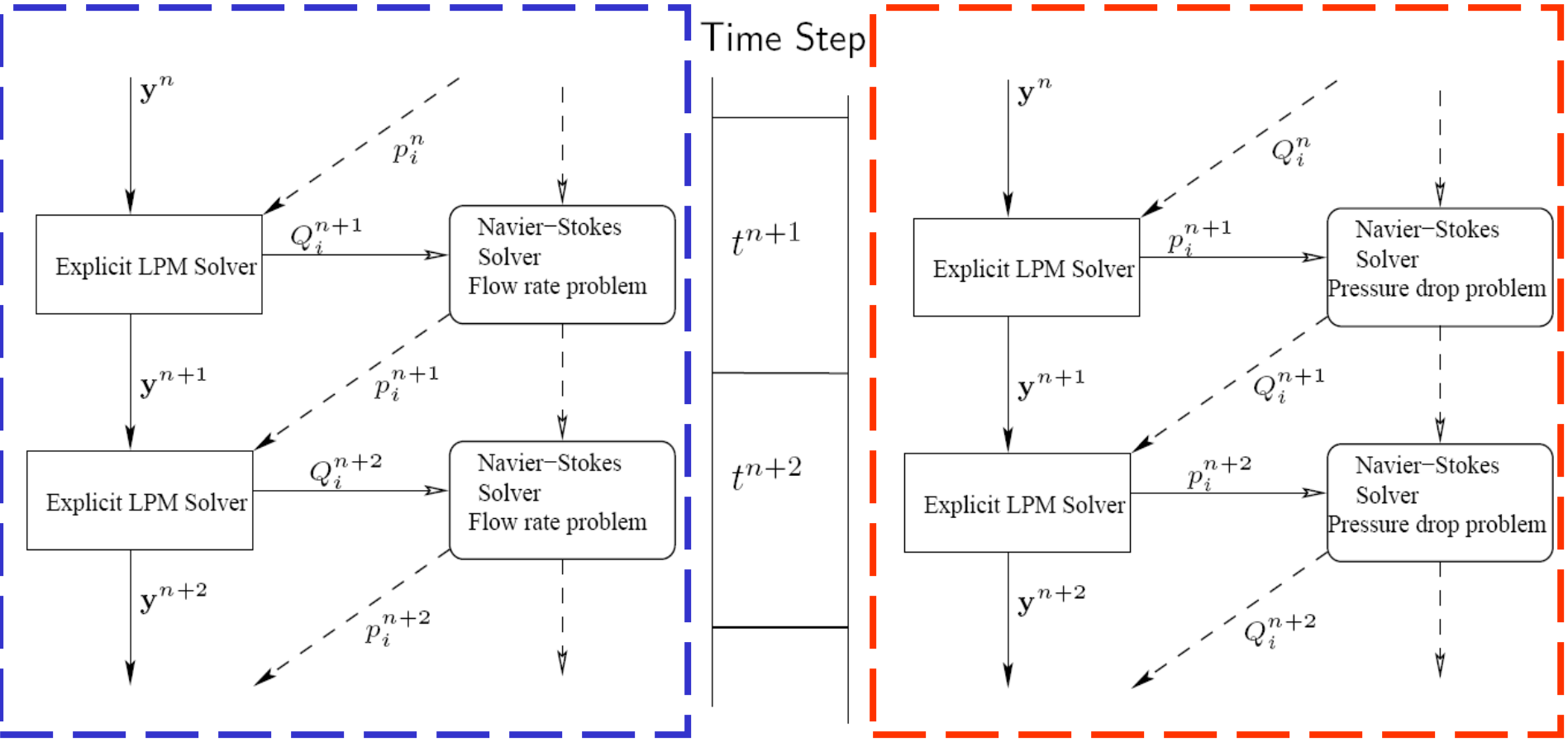

Simulation of a by-pass anastomosis

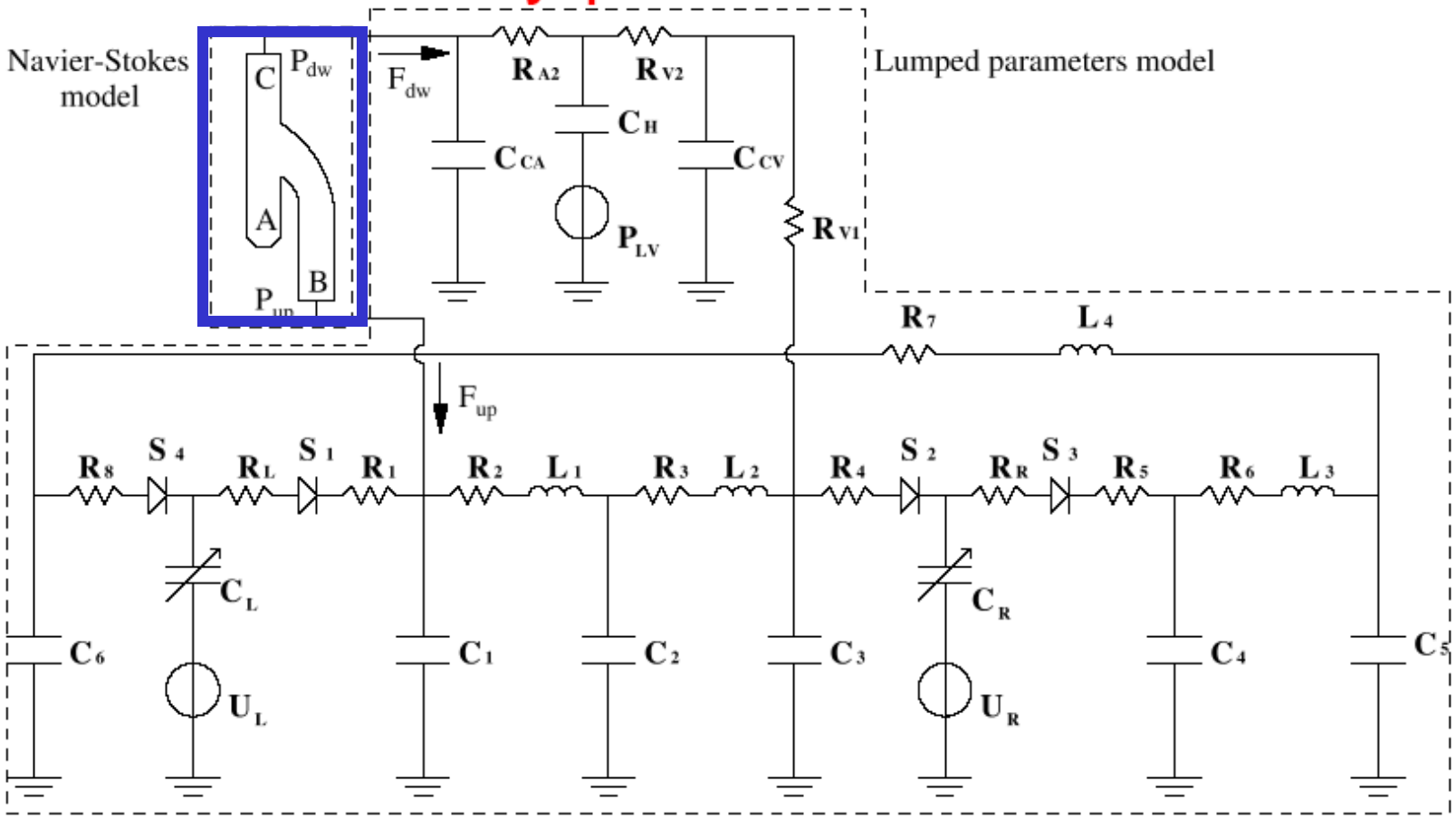

Simulation of a by-pass anastomosis

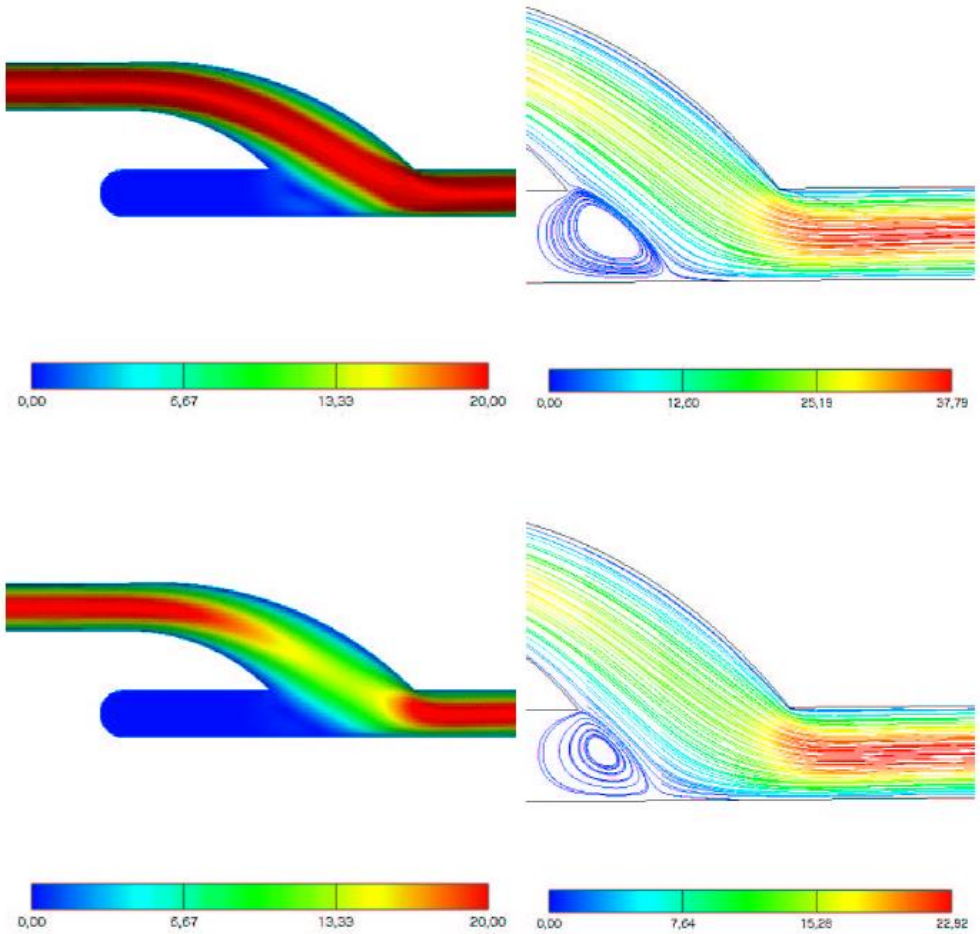

Velocity and contour and streamlines plots at a quarter and at the end of a heart beat.

Simulation of a by-pass anastomosis

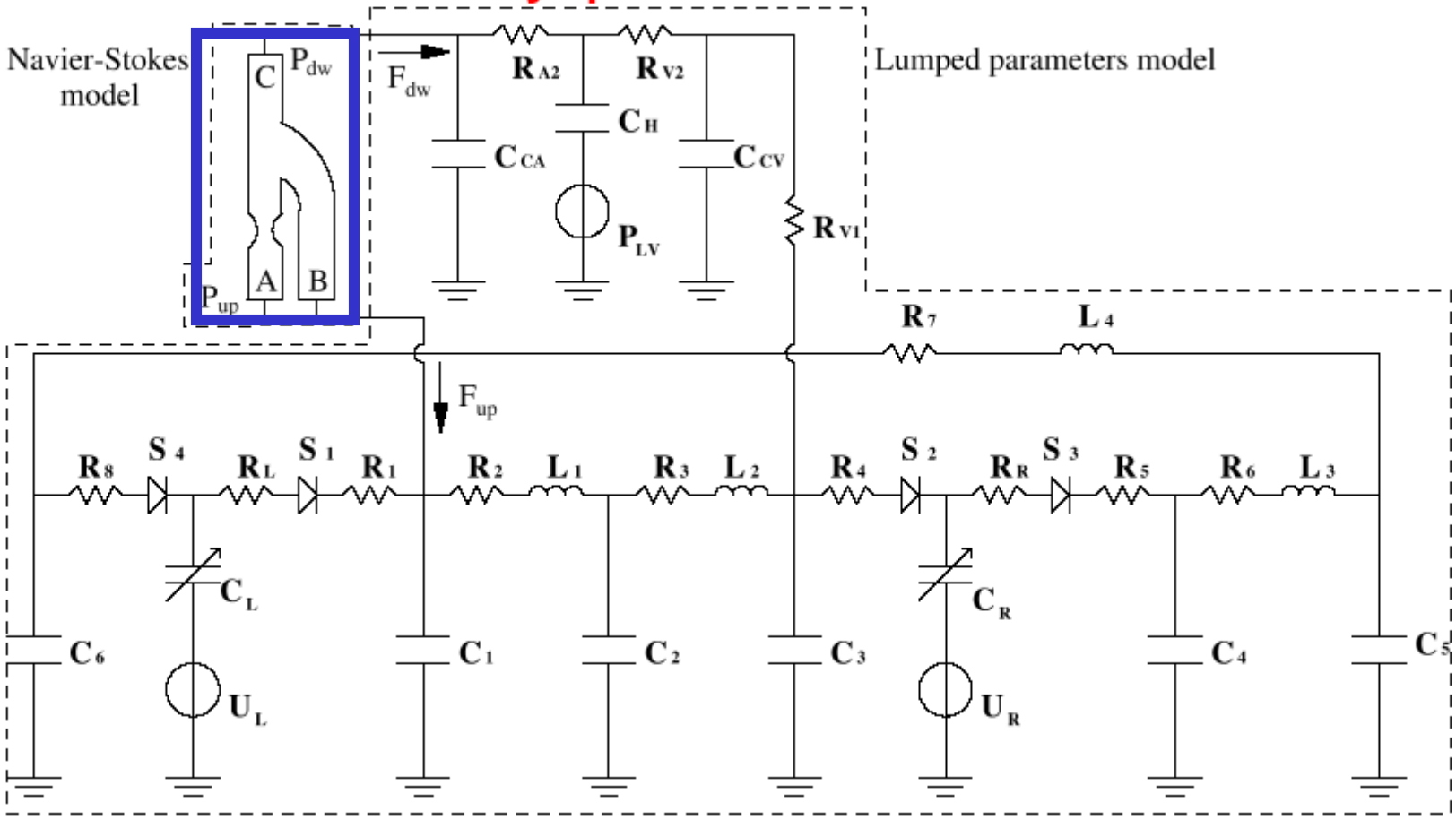

Simulation of a by-pass anastomosis

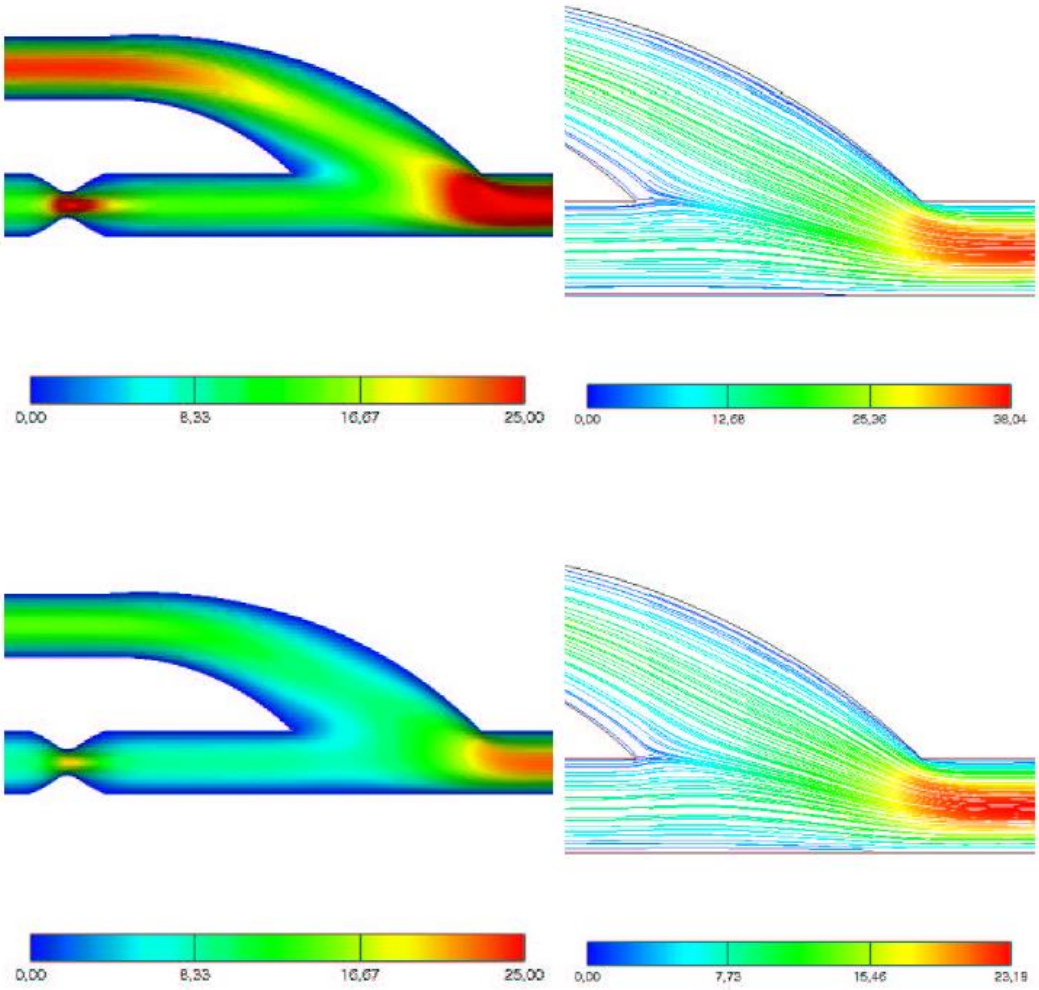

Velocity and contour and streamlines plots at a quarter and at the end of a heart beat.

Simulation of a by-pass anastomosis

Comparison between the flux distributions in the totally occluded and partially occluded cases.

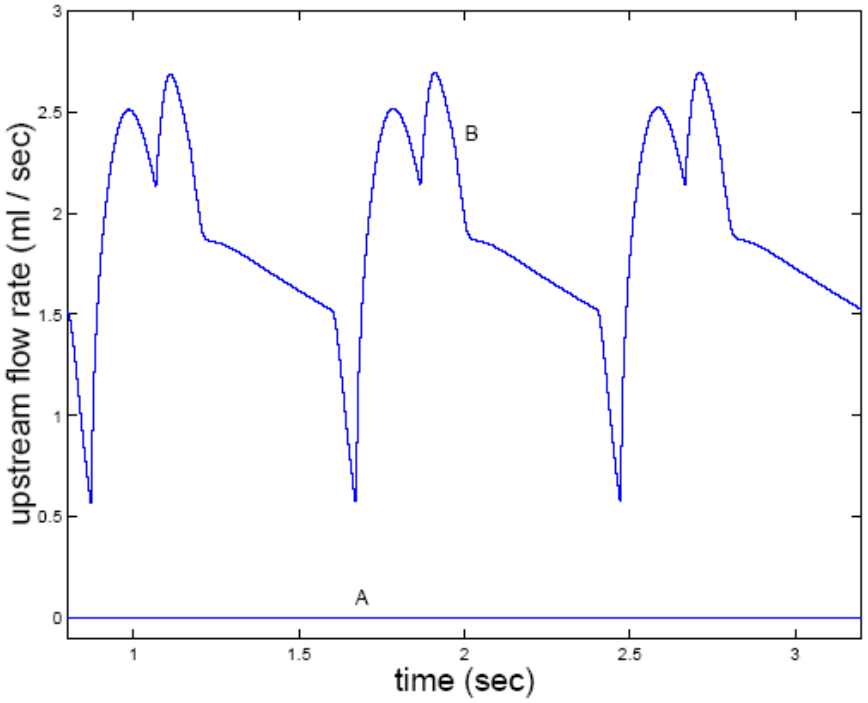

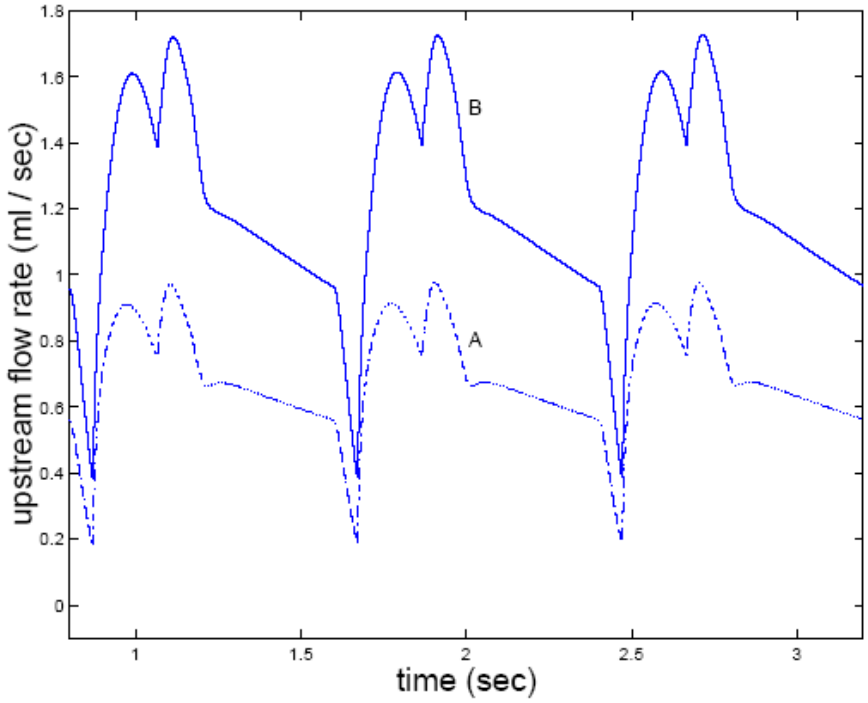

Coupling Algorithms III: 3D/1D

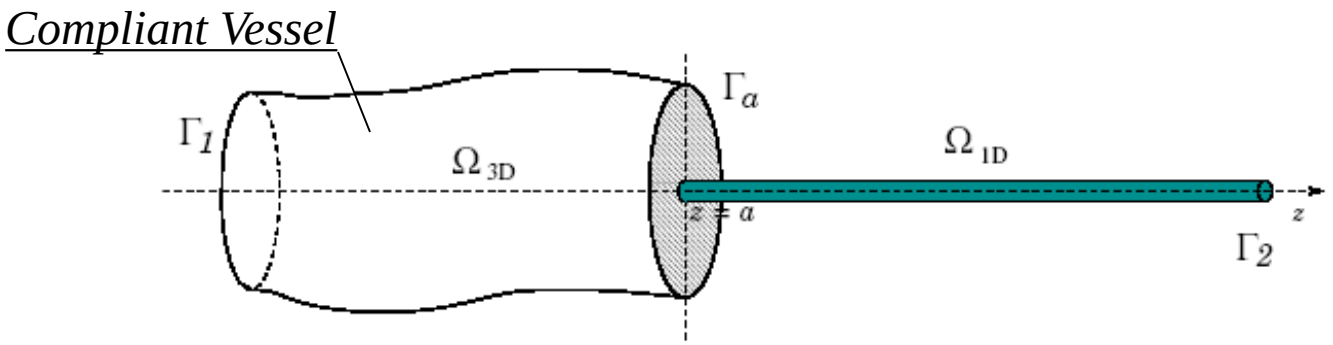

In the coupling between 3D and 1D models we have more possibilities at the interface.

Possible Interface Conditions (not linearly independent):

[A] Area $A(a^-) = A(a^+)$

[B] Averaged Normal Stresses $\bar{\sigma}(a^-) = \bar{p}(a^+)$

[C] Flux $Q(a^-) = Q(a^+)$

[D] Incoming Characteristic $\overline{u}(a^-) + 2\sqrt{\frac{2}{\rho}}\left(\sqrt{\bar{\sigma}(a^-) - p_{ext} + p^*)} - \sqrt{p^*}\right) = W_1(a^+)$

Actually, it is possible to see that [A], [B], [D] implies [C]

A possible algorithm

Time step $n+1$: solution at t^n is given. It provides an initial guess for the solution at t^{n+1}.

Loop on k: iterate up to the fulfillment of a convergence test:

1. From the velocity, pressure, area solution at the iteration k compute W_1 at the interface and solve the 1D model with condition [D]. 1D computation provides the new estimate for area (pressure).
2. Compute the 3D model, imposing condition [A] and [B], yielding a new estimate for W_1

Remark

- Due to the mismatch between the structure treatment of the two models, some numerical instabilities can occur. An explicit scheme is not suitable.
- One or more relaxation parameters can improve the convergence
- A complete analysis of the interface conditions and coupling algorithms is still to be done

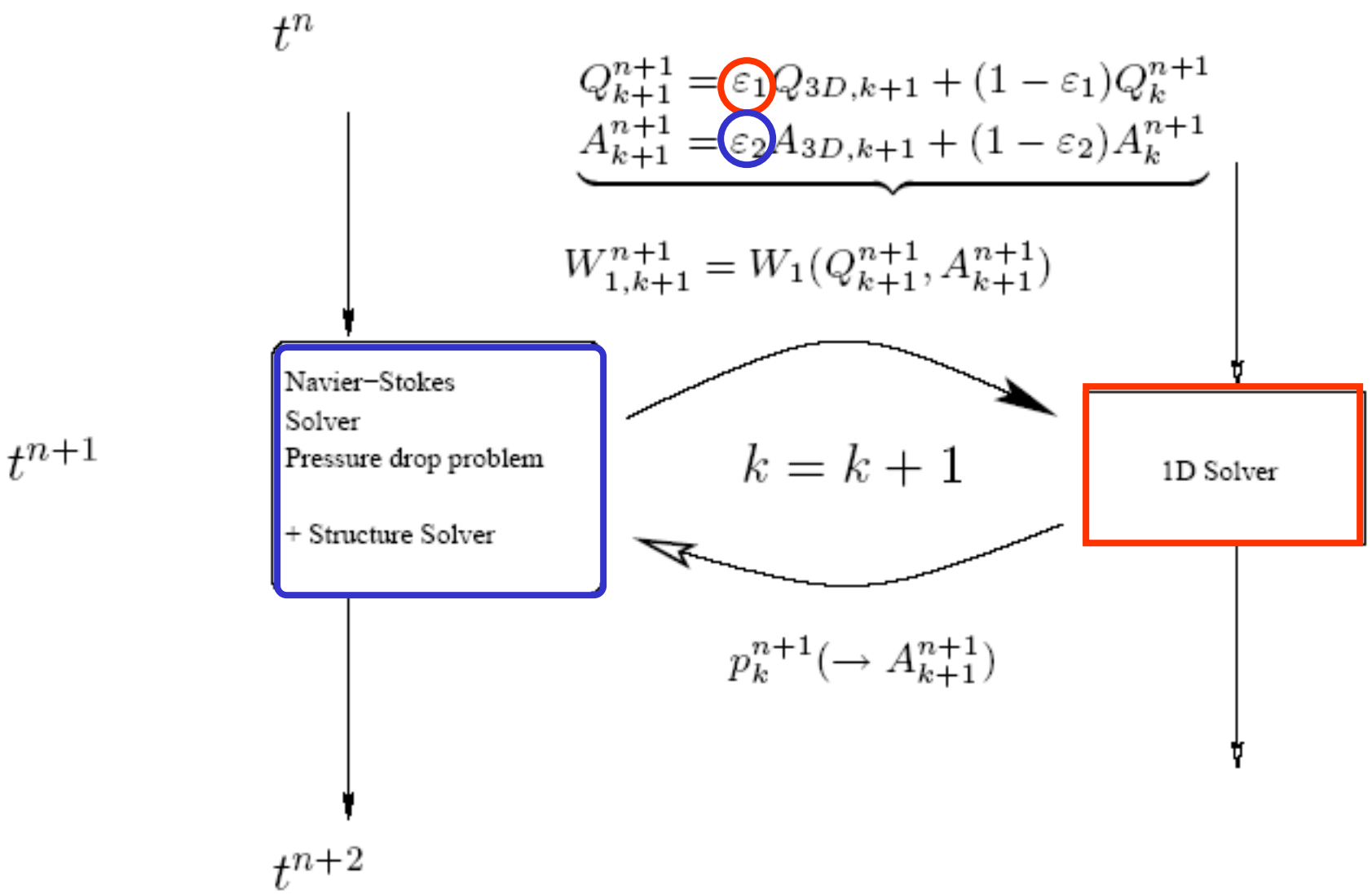

This algorithm has been used in the results shown in the previous lesson

First Example: 1D – LP Heart Model

Ackn:L. Formaggia, D.Lamponi, M. Tuveri

Tasks:

1. to simulate pressure wave propagation in the 55 largest arteries **(1D model)**;

2. to account for the presence of the heart and the peripheral circulation **(0D model)**;

3. to simulate pathological occlusions (from 55 to 53 arteries).

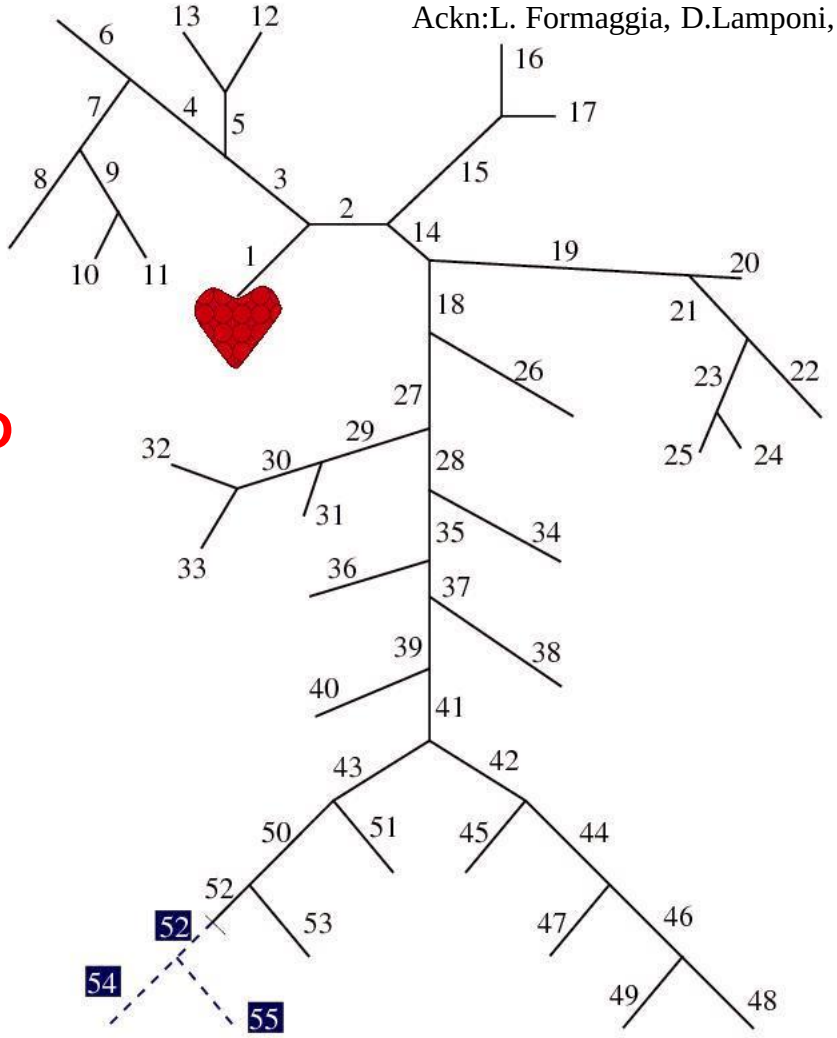

Network taken from Wang, Parker, 2004, Sherwin, Peirò, Franke 2003

Issues:

Heart Lumped Parameter model

Heart/Network Coupling

Peripheral Circulation

"The left ventricle and arterial circulation represent two mechanical units that are joined together to form a coupled biological system". McDonald's Blood Flow in Arteries, 1998.

Standard heart modeling:

The heart is described as a boundary inflow condition to the arterial network.

No feedback from the arterial system to the heart.

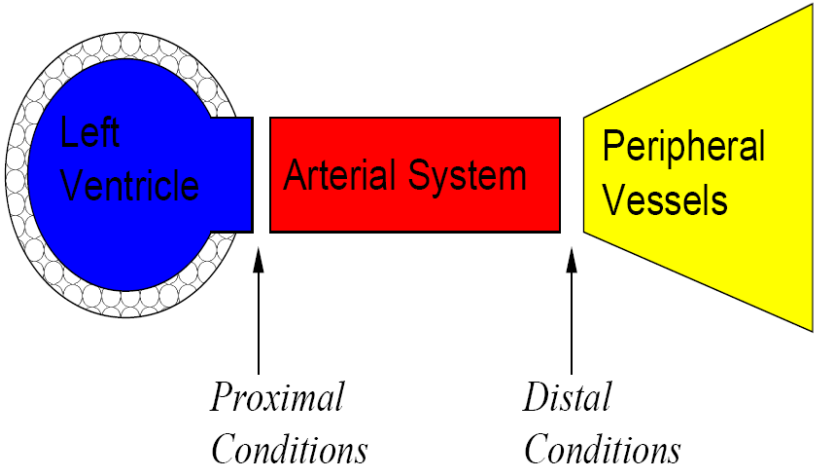

Multiscale modeling: lumped parameters description of the heart (McD's Blood Flow)

Pressure and volume in the left ventricle are linked together through the time-dependent *elastance*

Cardiac elastance is low during the diastolic phase and increases during the systolic one.

$$P_v(t) = E_v(t)(V_v(t) - V_0) + KE_v(t)(V_v - V_0)Q_v(t)$$

(P_v = ventric. press., V_v = ventric. vol., V_0 = ref. volume, K= resist. coeff.)

Heart/Arterial System Coupling

Assumptions: aortic valve opens under the pressure difference action, and closes under the action of a flow reversal.

Closed valve conditions (Diastolic phase):

$Q_V = 0$

(in terms of Riemann invariants: $W_1 = -W_2$)

Valve Opening: when $p_{arterial} < P_V$

Open valve conditions (Systolic phase)

Continuity of pressure and flux:

Solve for P_V:

$$\frac{1}{E}\frac{dP_V}{dt} + \frac{d}{dt}\left(\frac{1}{E}\right)P_V = -Q_V$$

where Q_V is computed from the network.

Valve Closure: when $Q_V < 0$

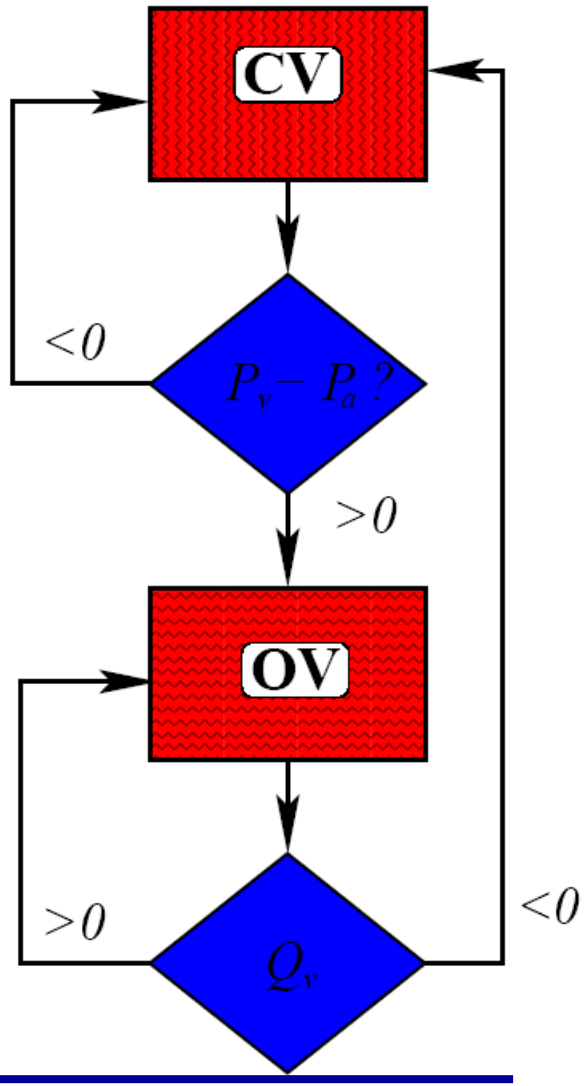

Peripheral Circulation

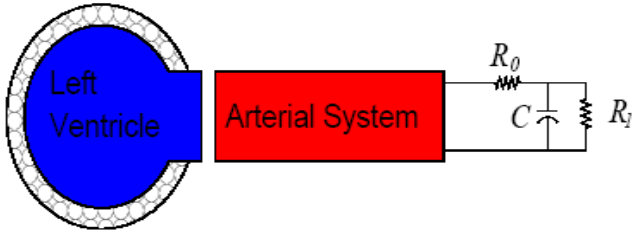

Standard approach:

distal circulation lumped in a purely resistive load:

$$p = RQ$$

Present approach: three elements Windkessel downstream vessels:

$$p + R_1 C \frac{dp}{dt} = R_p Q + R_0 R_1 C \frac{dQ}{dt}.$$

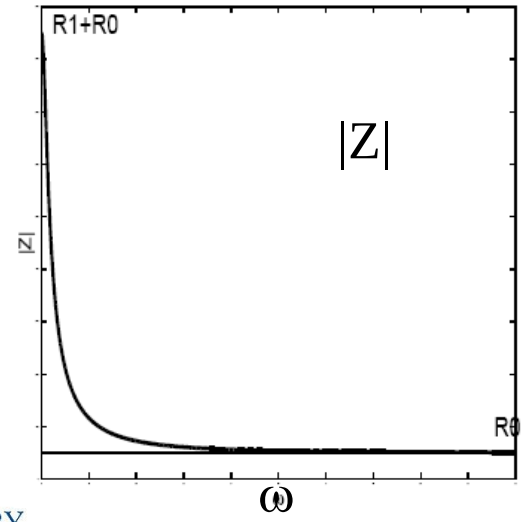

Windkessel Impedance:

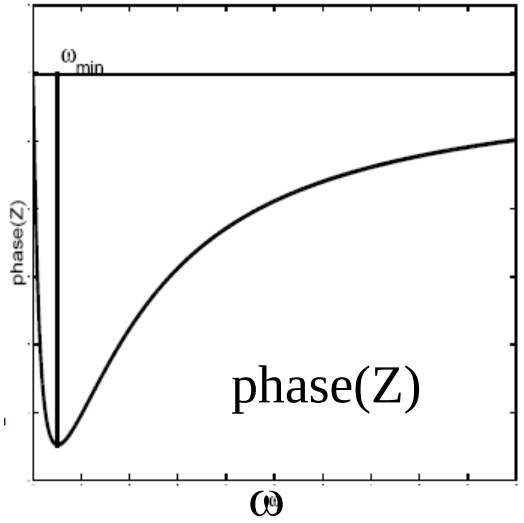

Impact of the heart coupling: adult patient

Left: without coupling **Right: with coupling**

Thoracic Aorta

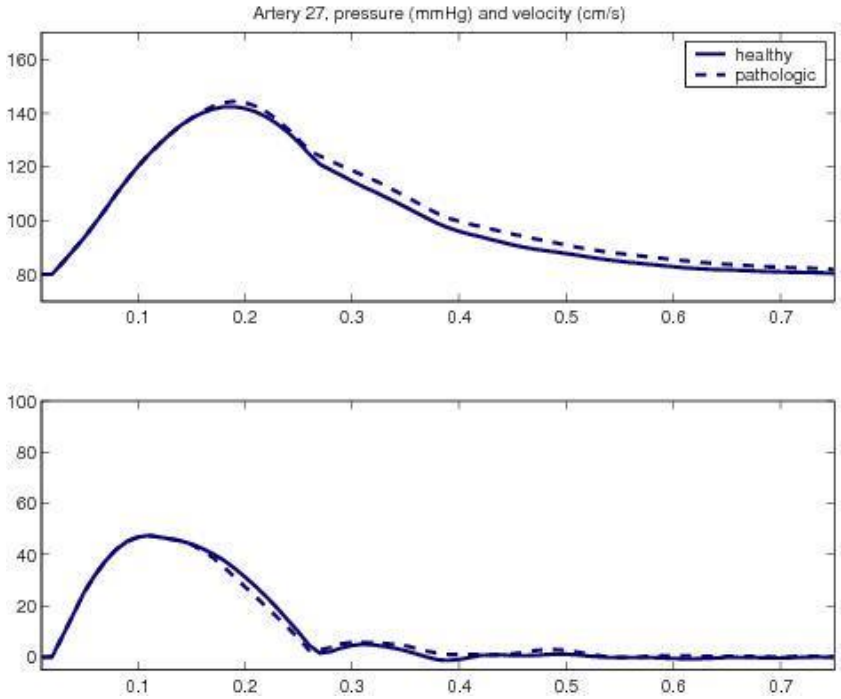

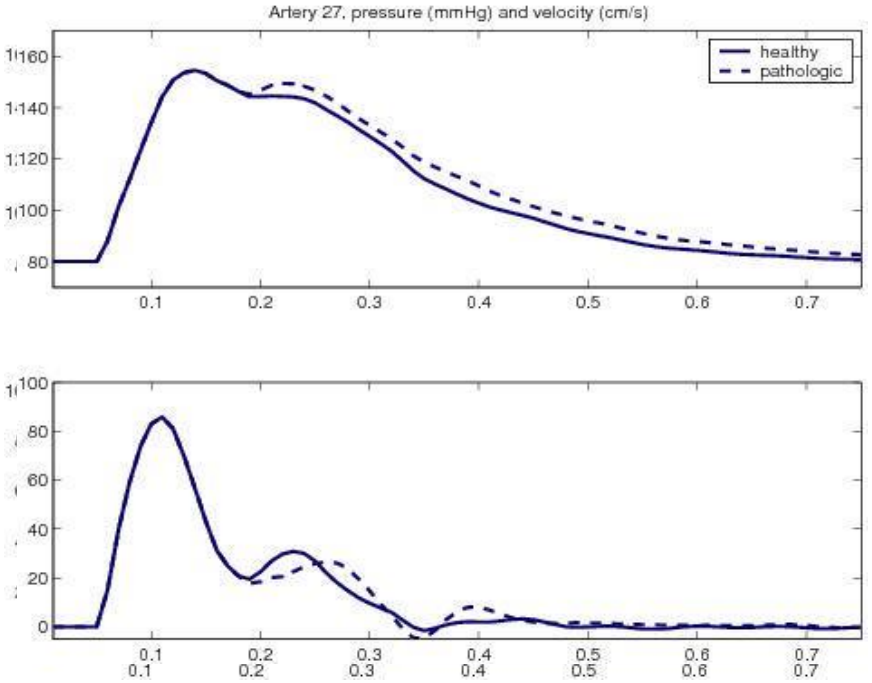

The traditional approach underestimates the wave reflections, since the heart working is actually independent of the arterial feedback. *This is particularly evident in the pathological case (reflections induced by the occlusion)*.

Impact of the heart coupling: elder patient

Left: without coupling *Thoracic Aorta* **Right: with coupling**

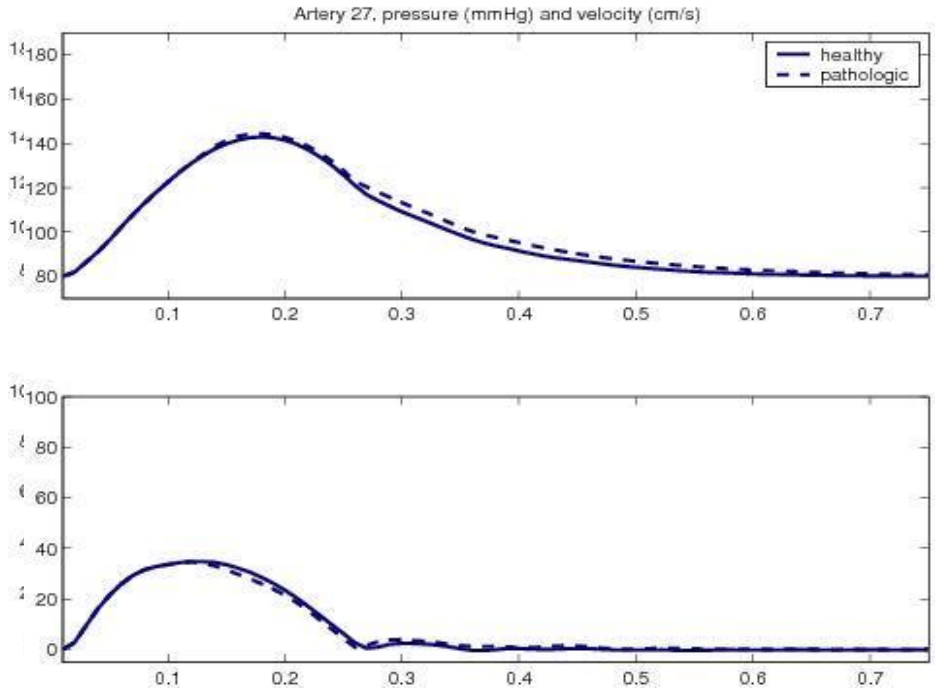

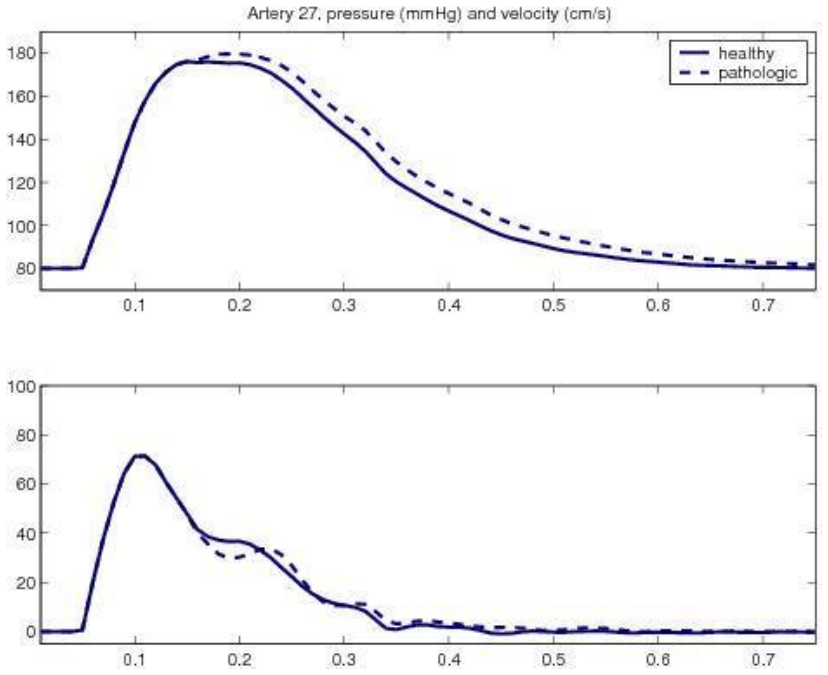

In an *elder patient* we assume a doubled arterial Young modulus (stiffening). The traditional approach underestimates the sensitivity to the arterial stiffness.

Multiscale simulation of aging effects

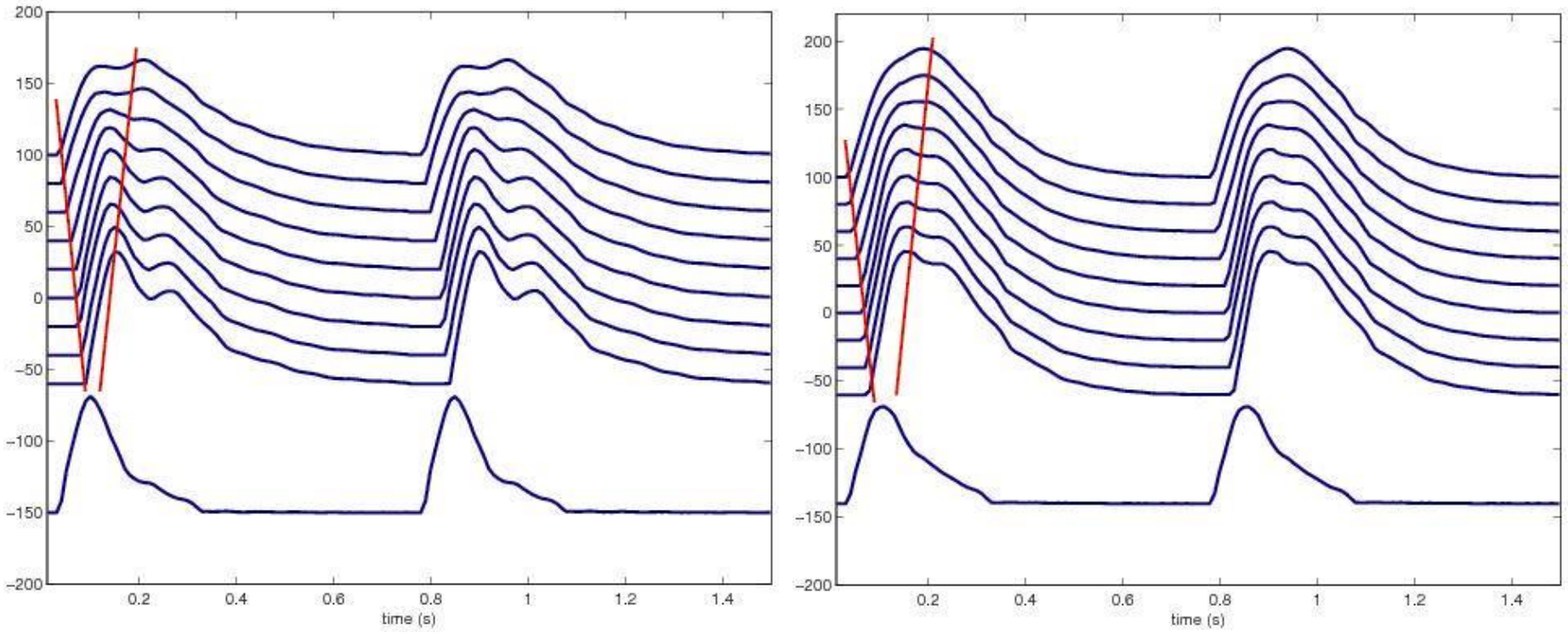

Pressure waves at different locations (from ascending aorta to iliac bifurcation) for a middle aged (left) and an elderly patient (right). On the bottom: the flow rate in the ascending aorta.

Onset of backflow and pressure increment induced by the distal occlusion

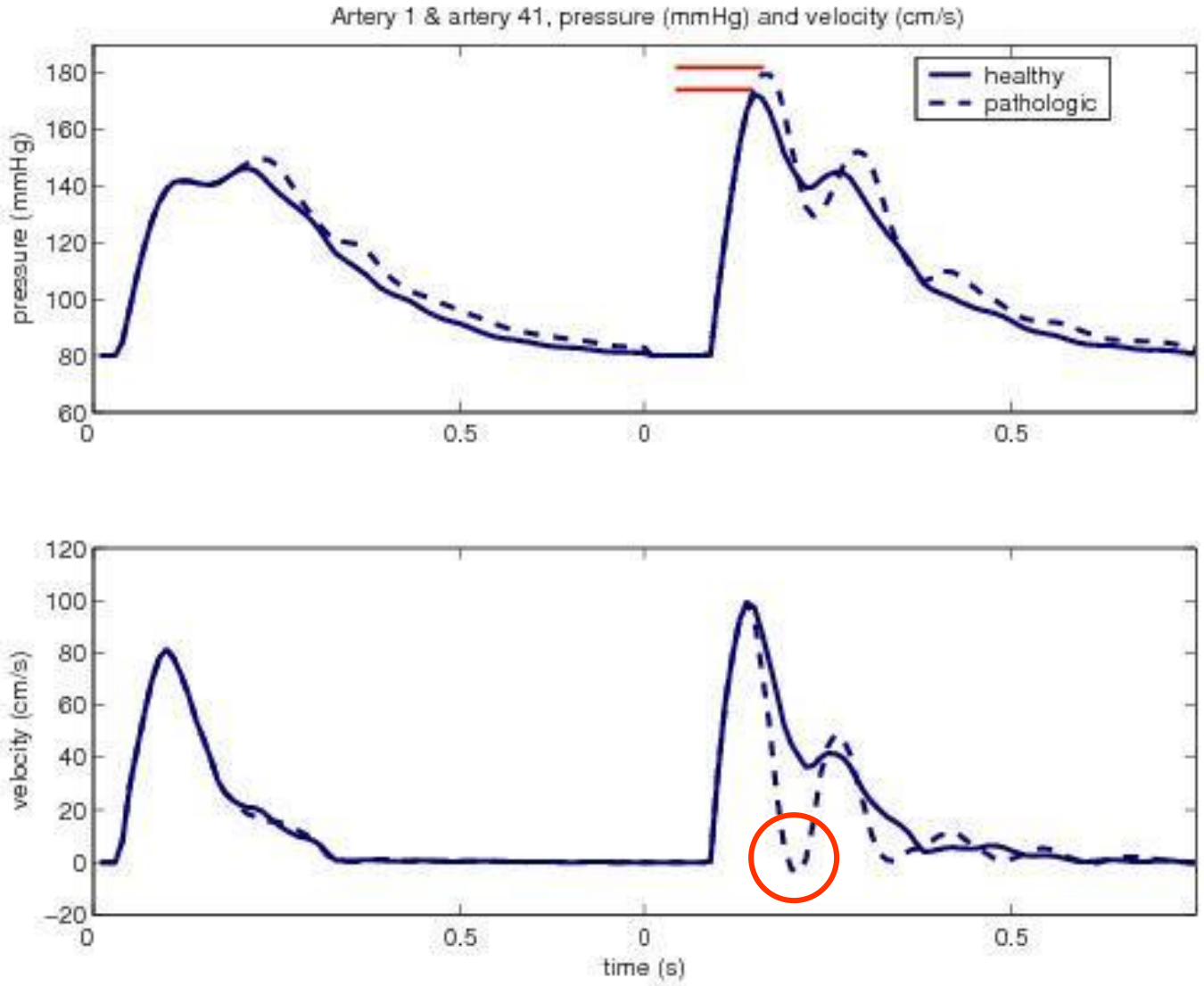

Second Example: Multiscale Carotid

R. Balossino et al. 2009

Application of the geometrical multiscale methodology to the investigation of the fluidynamic behaviour of a carotid artery bifurcation

The choice of the carotid artery has been made because:

- it is an area particularly prone to plaque deposition with the danger of embolism
- it allows to highlight the importance of prescribing realistic boundary conditions

The final aim of the work is to investigate the impact of the multiscale approach on numerical simulations

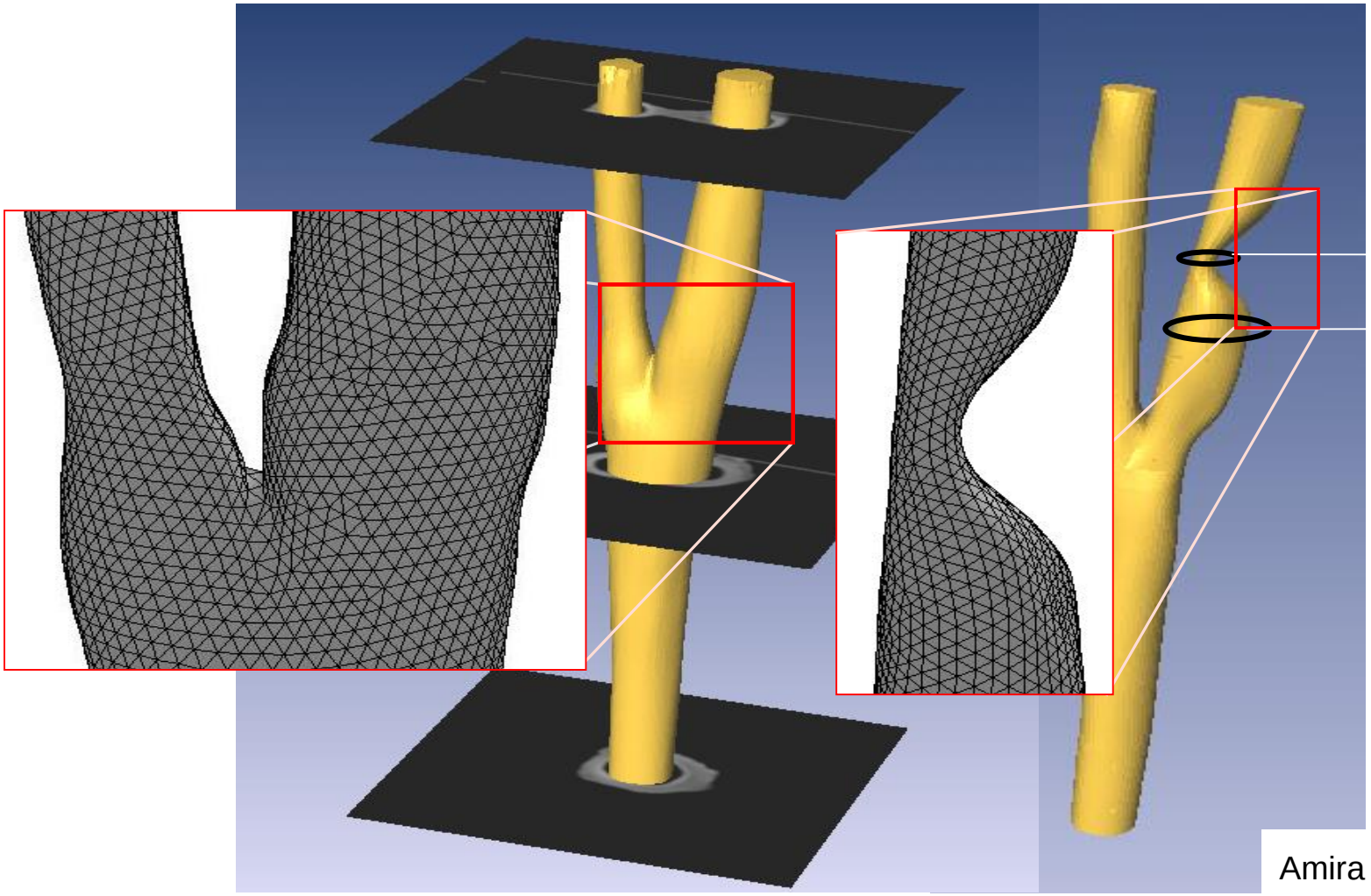

Diameter of the common carotid artery = 6.4 mm

Unstructured grid ≈ 100000 elements

Multiscale model: equations

3D Model: Incompressible Navier-Stokes Equations for an Incompressible Fluid

$$\begin{cases} \dfrac{\partial \mathbf{u}}{\partial t} + (\mathbf{u}\cdot\nabla)\,\mathbf{u} - \nu\Delta\mathbf{u} + \nabla p = \mathbf{f}(\mathbf{x},t) \\ \nabla\cdot\mathbf{u} = 0 \end{cases}$$

$\mathbf{u} = \mathbf{u}(\mathbf{x},t)$ is the velocity field;

$p = p(\mathbf{x},t)$ is the (kinematic) pressure;

0D Model: Compartment model. For each compartment a set of Ordinary Differential Equations is obtained by a space average of momentum and mass conservations (+ constitutive laws)

$$\begin{cases} C\dfrac{dP_2}{dt} - Q_1 = Q_2 \\ L\dfrac{dQ_1}{dt} + RQ_1 + P_2 = P_1 \end{cases}$$

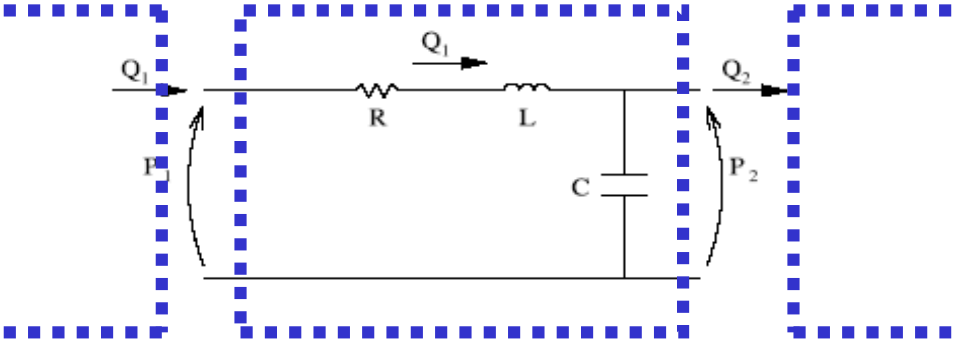

The whole lumped parameter model is described by a system in the form: $\dfrac{d\mathbf{y}}{dt} + A(\mathbf{y})\mathbf{y} = \mathbf{b}$

The ODE system was solved with an explicit Euler method, through a user defined function (UDF) included in the Fluent code (Fluent Inc, Lebanon, NH, USA)

Multiscale model: diagram

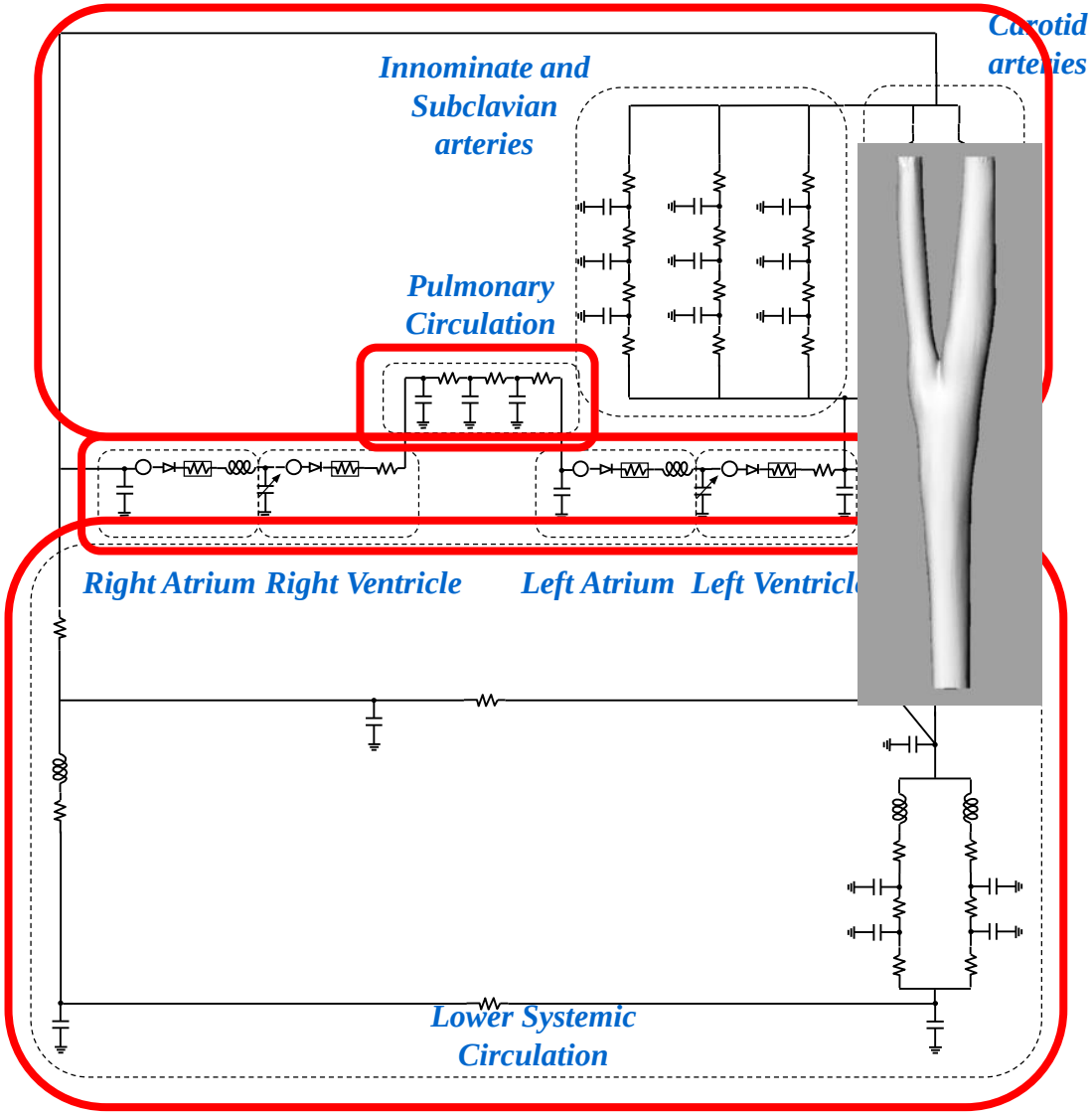

NS = Navier Stokes Model

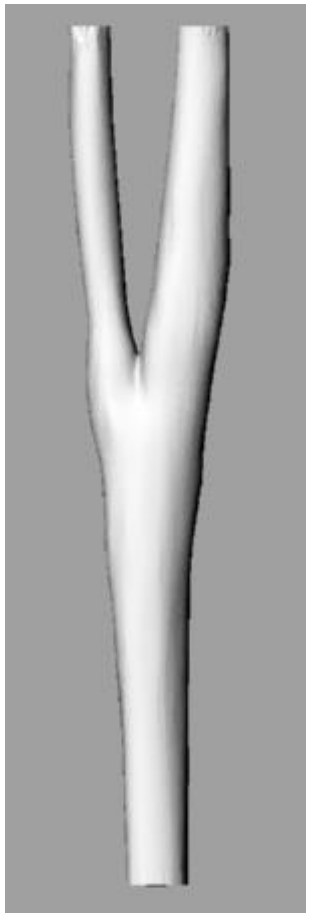

Absence of stenosis

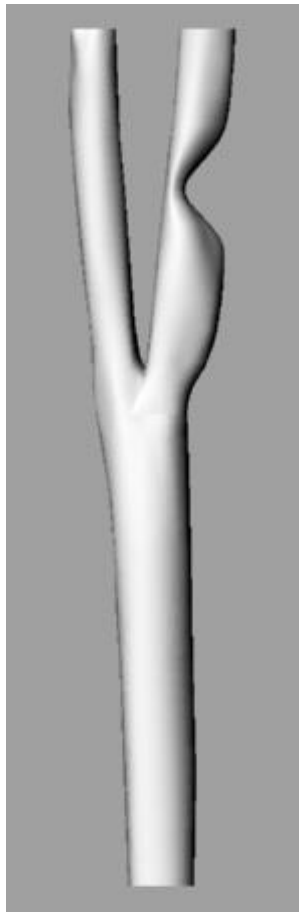

Presence of stenosis

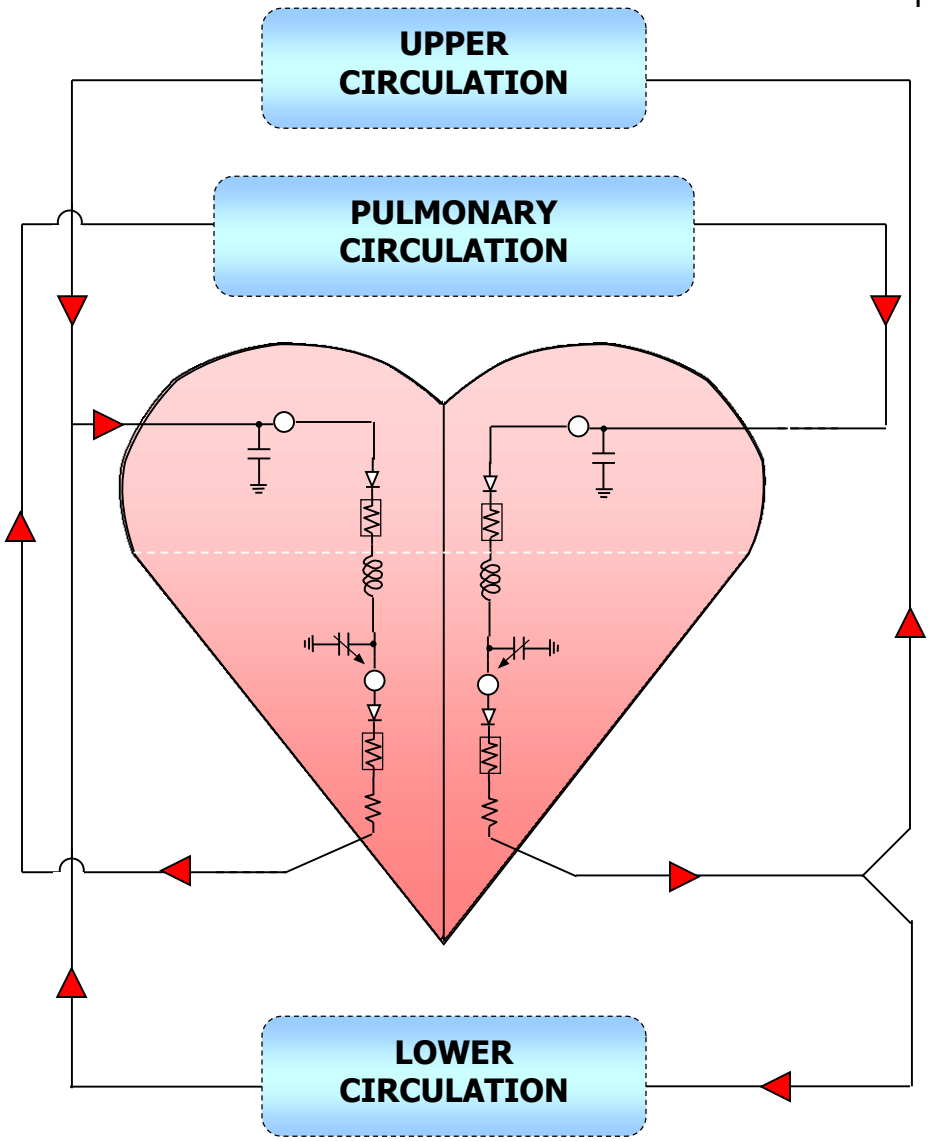

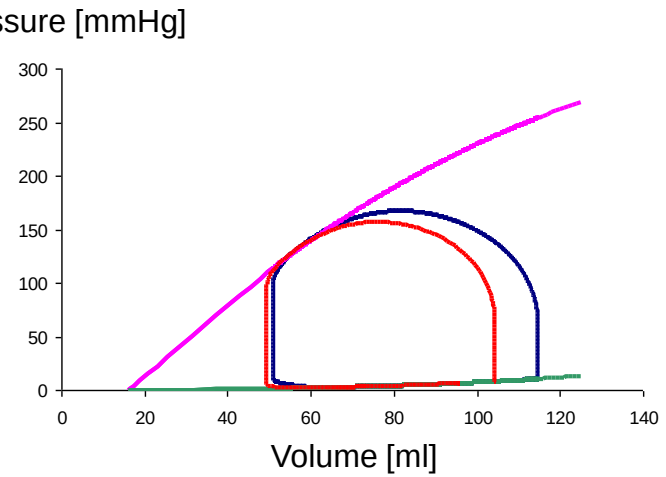

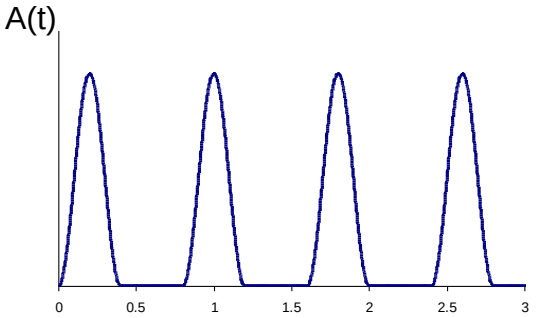

$$p_i(t) = p_i^a(t) + p_i^b(t)$$

$$p_i^a(t) = A(t) \cdot \left[U_i^0 + E_i^{sys}(V_i)\, V_i(t) \right]$$

$$p_i^b(t) = E_i^{dia}(V_i) \cdot V_i(t)$$

Multiscale model: numerical coupling

Semi-implicit approach

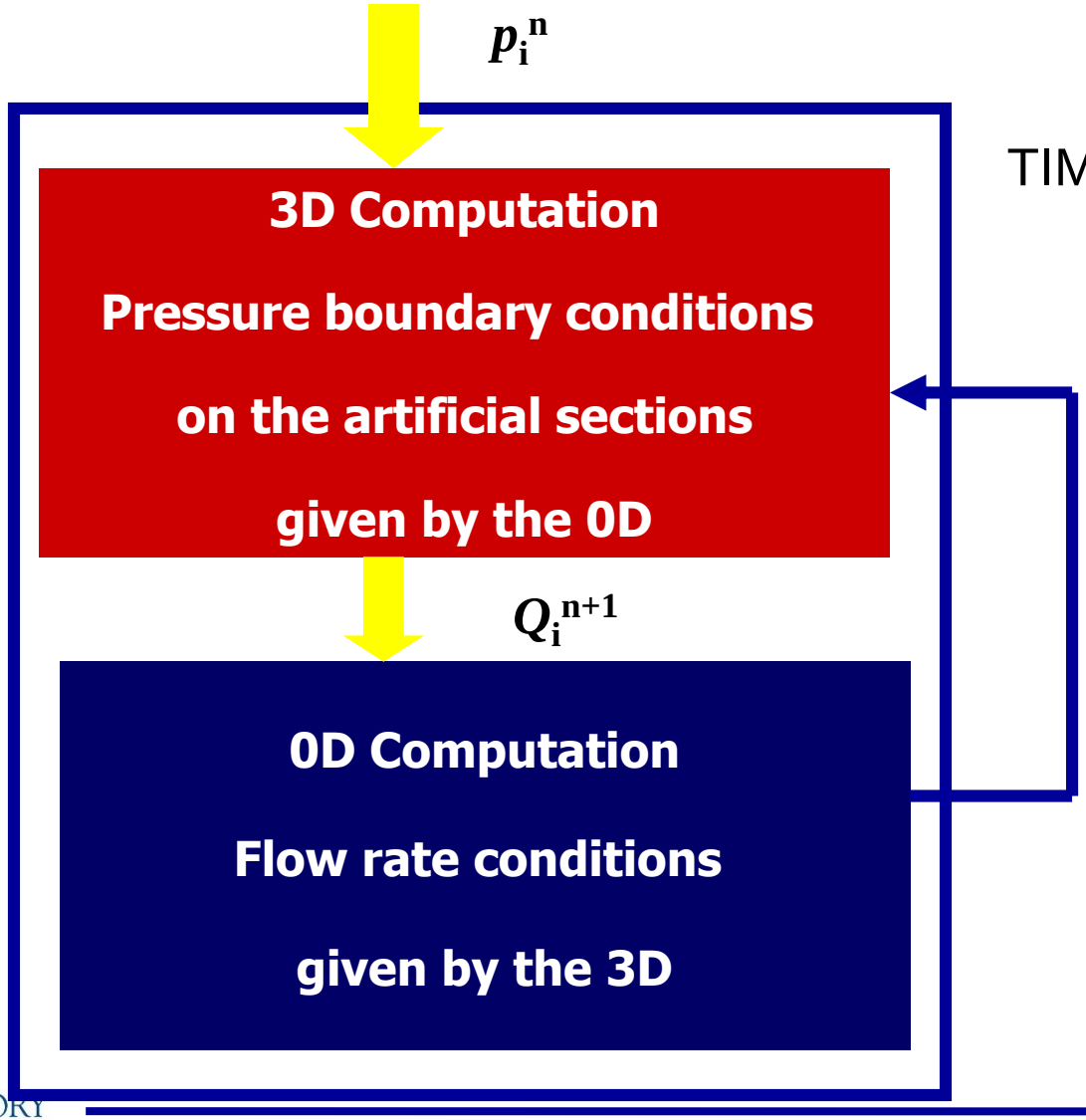

TIME STEP t^{n+1}

Sub-iterations (implicit approach)

Possible but actually not needed

Multiscale model: results

VELOCITY PROFILE

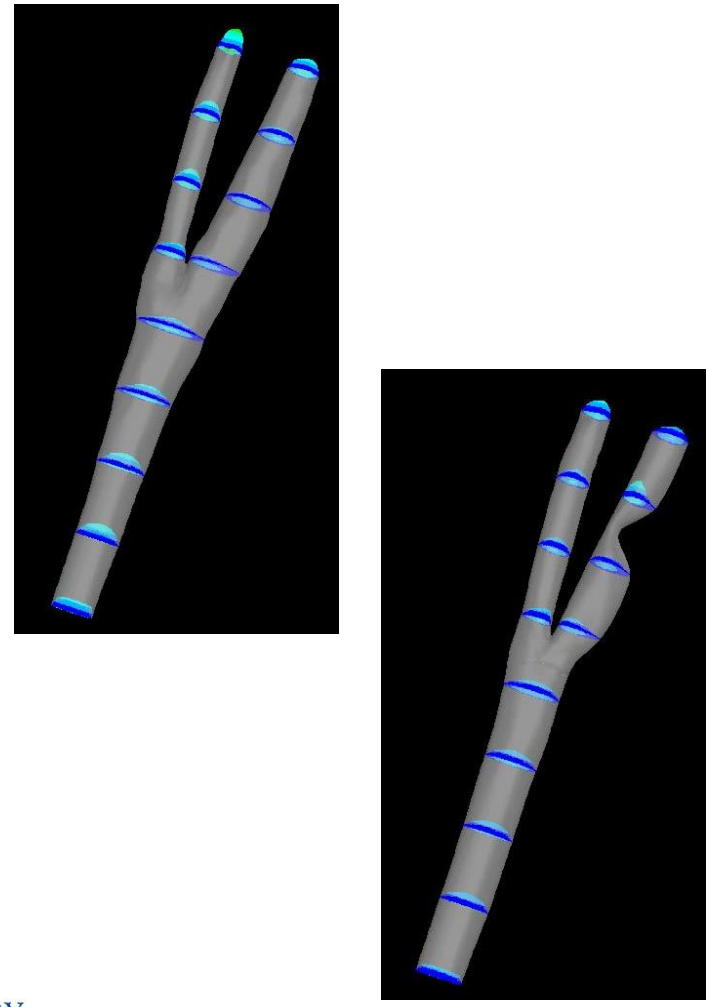

VELOCITY CONTOUR

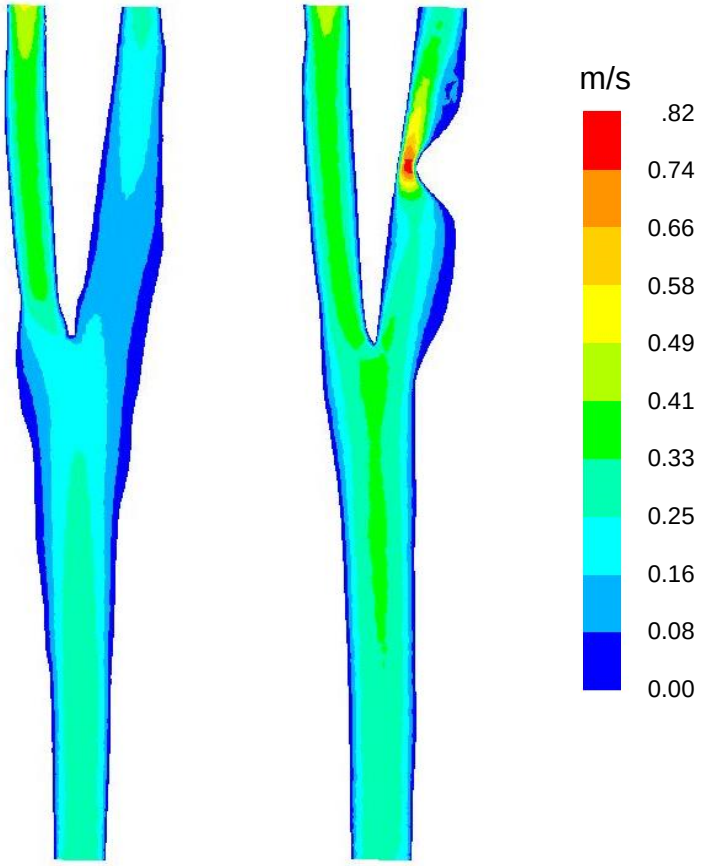

At systole (t = 0.2 s)

PRESSURE

TANGENTIAL WALL SHEAR STRESS

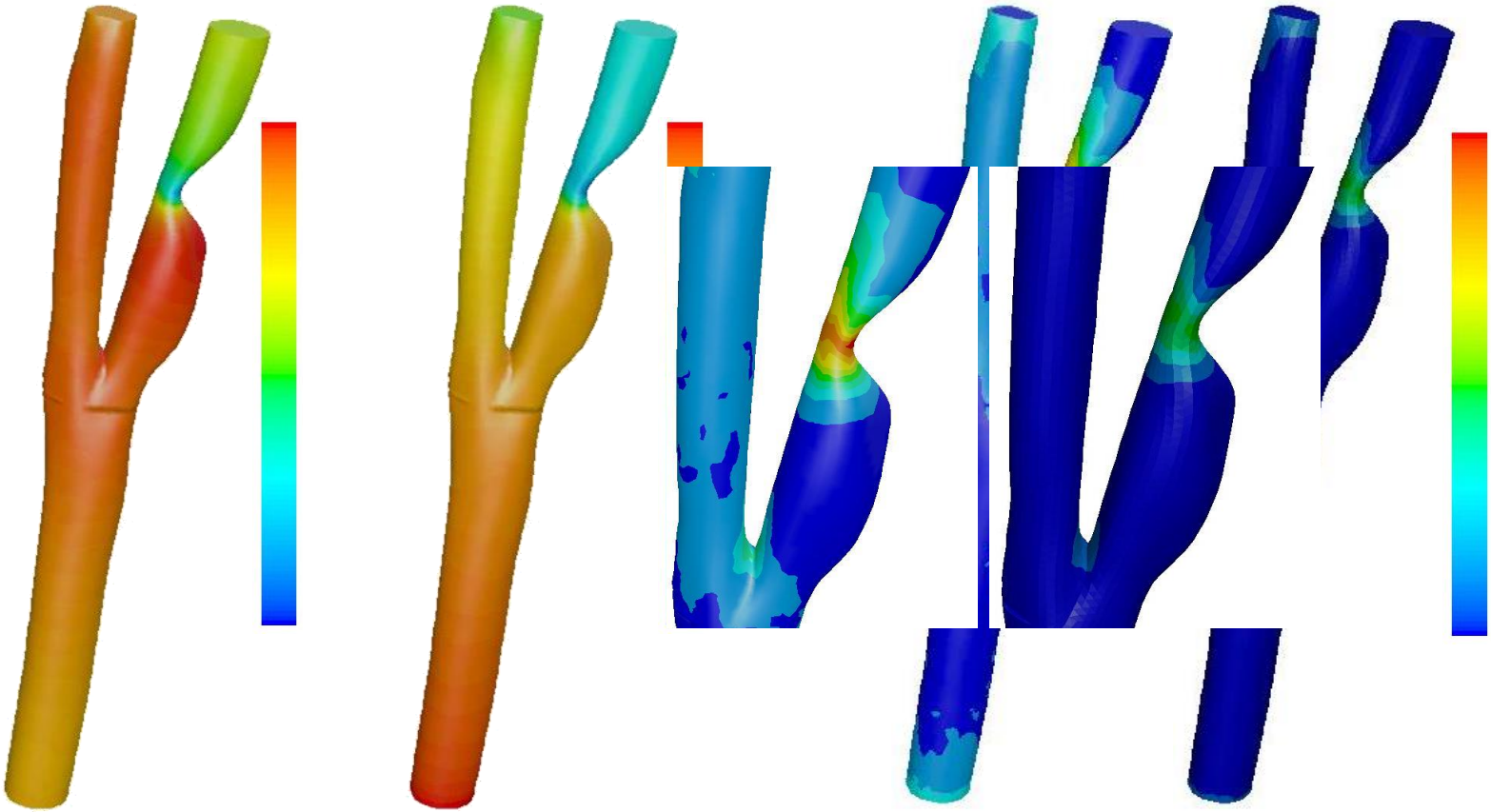

At systole (*t* = 0.2 s)

At diastole (*t* = 0.6 s)

At systole (*t* = 0.2 s)

At diastole (*t* = 0.6 s)

Presence of stenosis: almost equi-distribution in the two branches

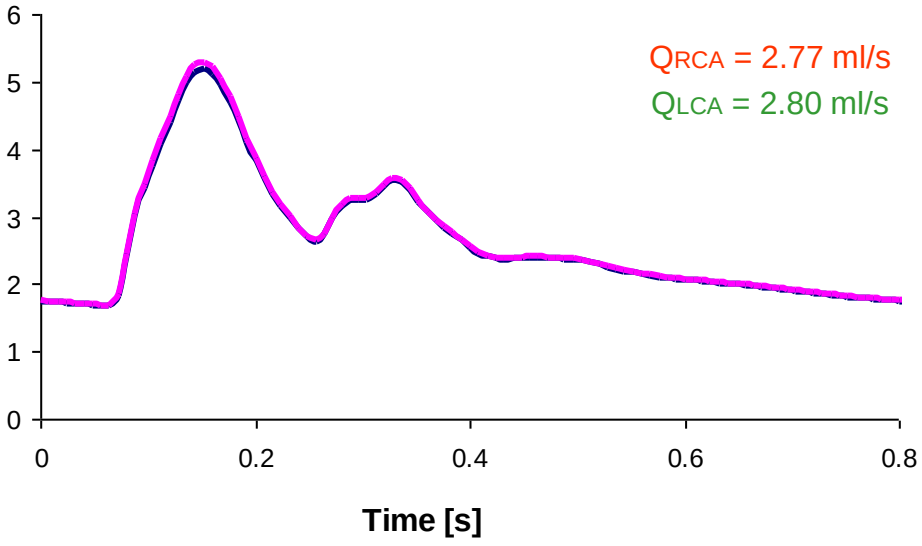

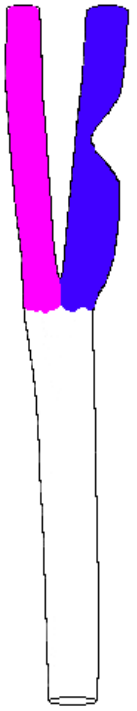

The results show that there are no significant differences between the flow distribution in the bifurcation with and without stenosis

Boundary condition:

- **Left and right carotid artery:** fixed and equal pressure
- **Wall:** no slip condition
- **Common carotid artery:** pulsatile velocity profile (resulting from the previous multiscale simulation)

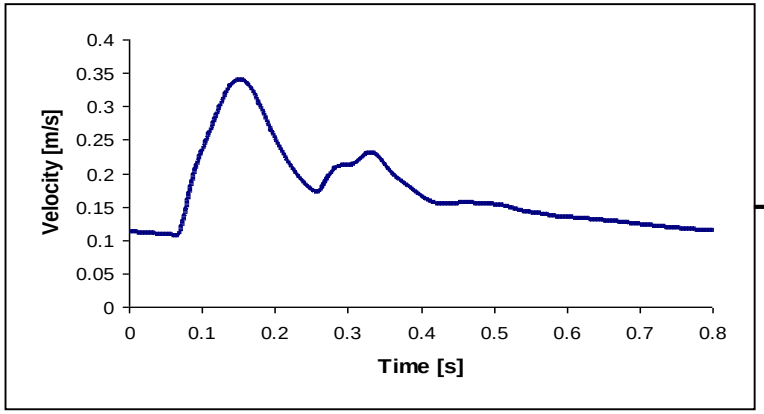

Cicle duration: 0.8 s

Heart-rate of 75 bpm

Stand-alone 3D model vs multiscale model

In the **stand-alone 3D** FVM the resistance caused by the stenosis is dominant, so for the same imposed outlet pressures, the flow rate is greater in the left branch respect to the right one.

In the **multiscale model** (LPM + FVM), instead, the resistances at the downstream of the two carotid branches are greater than that generated by the obstruction in the right branch. As a result, according to the relationship: $\Delta P = R*Q$, the flow rate in the two branches is almost the same.

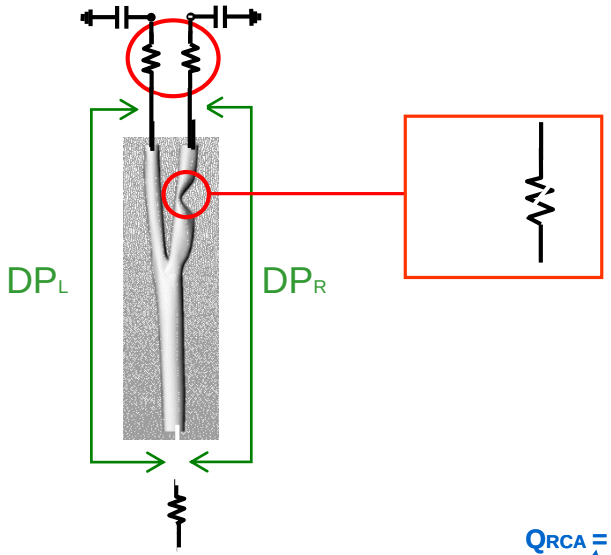

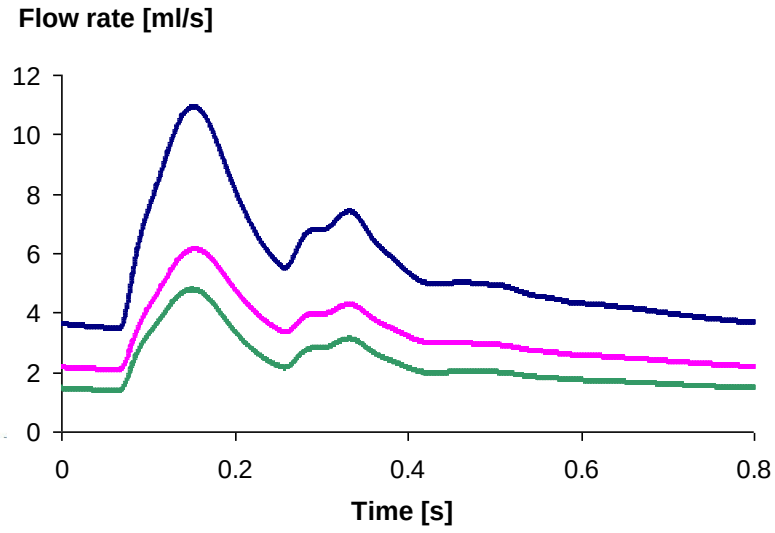

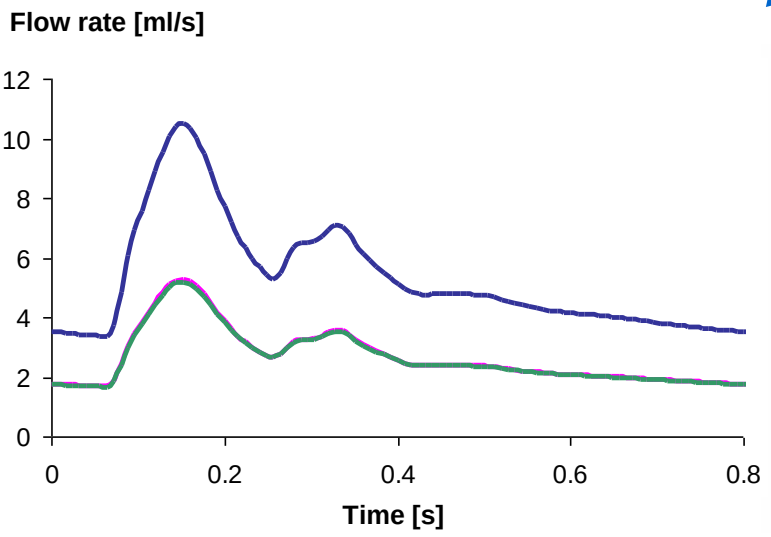

A non-standard application*

Problem: Propagation of pressure waves in the arterial tree and viscous blood motion *have different characteristic times* (S. Cănic).

1. In many bioengineering applications involving a 3D model over a few centimeters compliance can be neglected (for reducing CPU times)
2. In a multiscale network we are not allowed to neglect compliance for the effects over the tree and numerical instabilities (increment in CPU times)

A possible trade off (?): rigid 3D with "compliant" boundary conditions

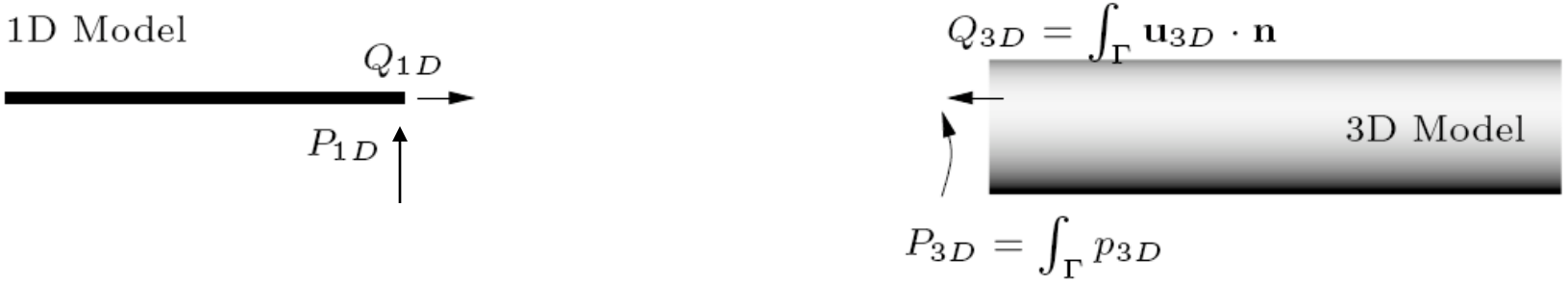

$$P_{1D} - R_1 Q_{1D} = P = P_{3D} - L\frac{dQ_{3D}}{dt} - R_2 Q_{3D}$$
$$C\frac{dP}{dt} = Q_{1D} + Q_{3D}.$$

$$C \propto \frac{A_0^{3/2} l}{E h_0}$$

*T.Passerini, MR. De Luca, L. Formaggia, A. Quarteroni, A. Veneziani (2008)

A non standard application (II)

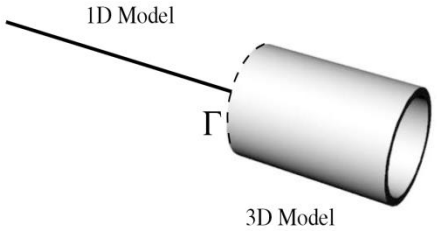

Sinusoidal flow rate
imposed on the inlet (left) section of 1D model

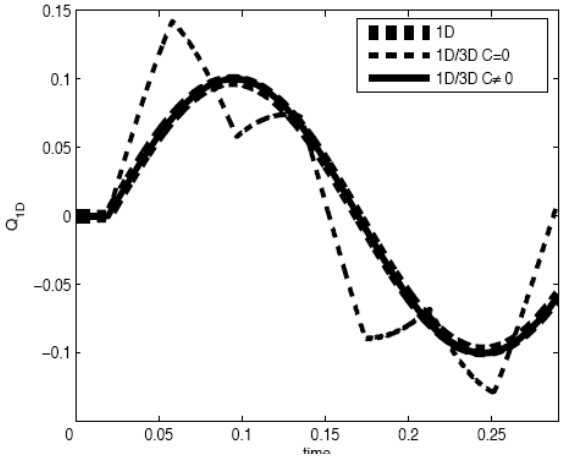

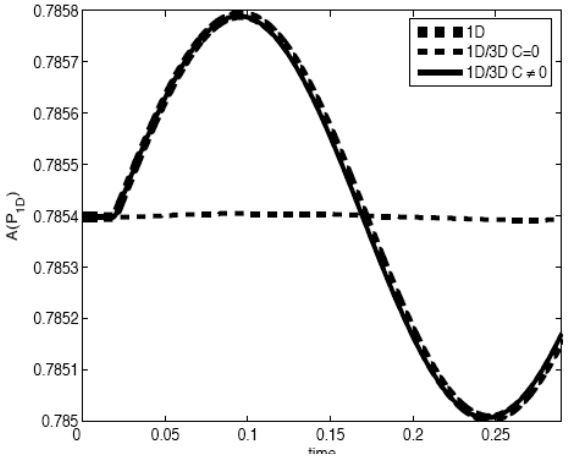

Plots show Q1D and Q3D on $\wp$ and comparison with a fully 1D solution evaluated on the corresponding node

Step flow rate
imposed on the inlet (left) section of 1D model

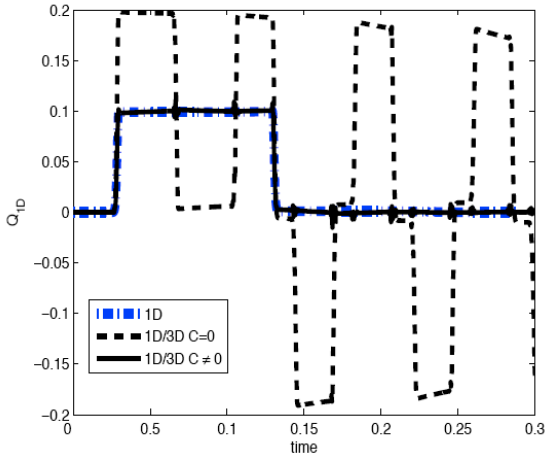

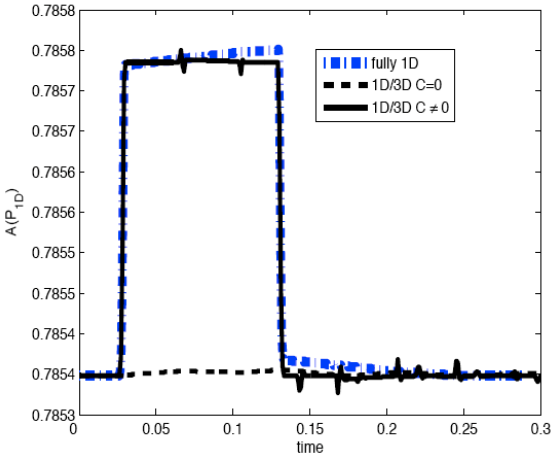

A non standard application (III)

(preliminary results)

1st RCL (l)

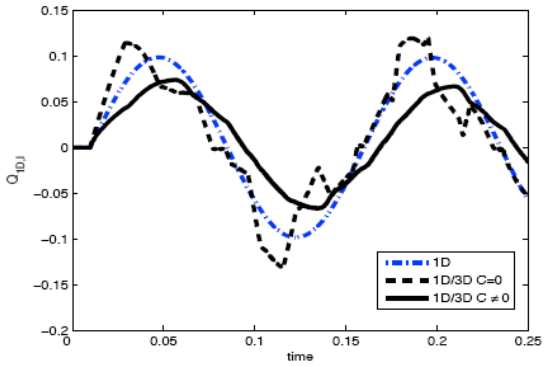

outlet section (end)

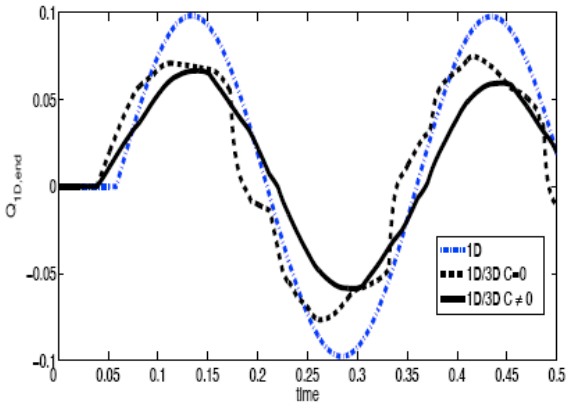

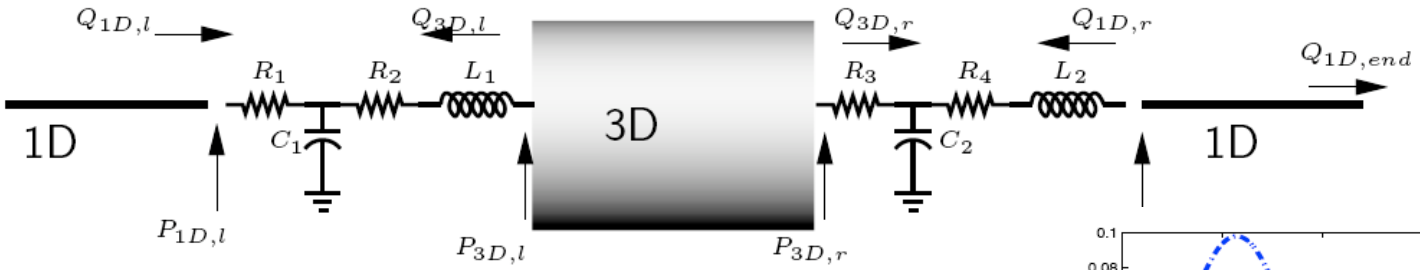

C1, C2 estimated from 3D model parameters

L1, L2, R2, R3 tuned with numerical experiments

R1, R4 characteristic impedance of 1D model

2nd RCL (r)

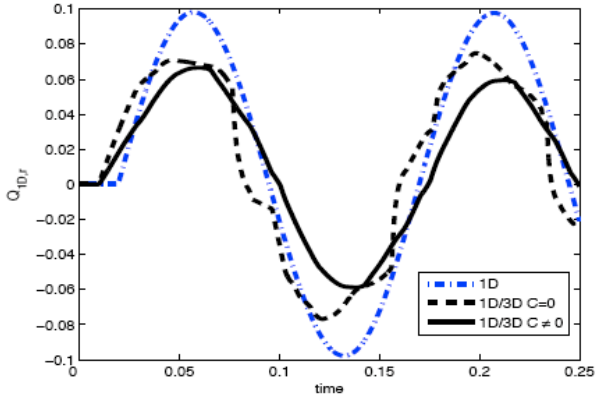

Conclusions

- The geometrical multiscale approach may provide a flexible paradigm for simulating the complex interactions of the cardiovascular system with a reasonable computational cost while being able to “refine” areas of interests;
- The velocity profiles are not prescribed a-priori and the clinical data comparison is good
- The same approach has been sucessfully “exported” in different contexts, e.g. river simulations, industrial combustion engines, cooling systems… even in an adaptive fashion (complicated!!!)

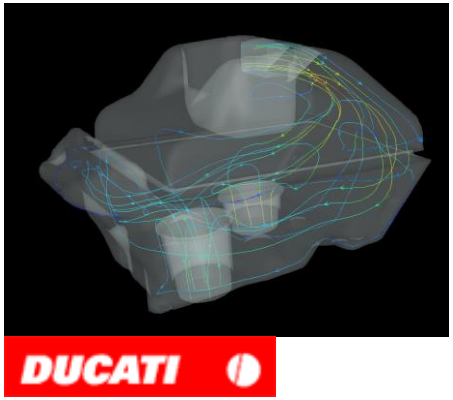

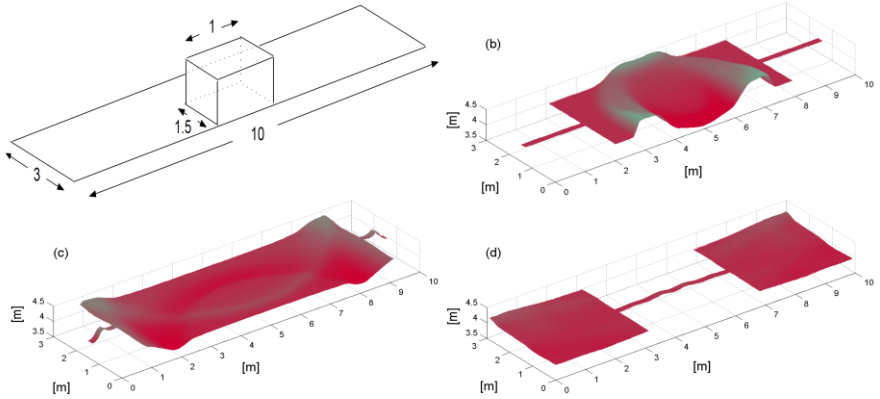

Fig. 2 Adaptive geometrical multiscale modeling: test case sketch (top-left); 3D representation of the free surface at $t = 1$s (top-right), $t = 2$s (bottom-left), $t = 10$s (bottom-right)

A comparison among Full/Geometrical Multiscale and HiMod

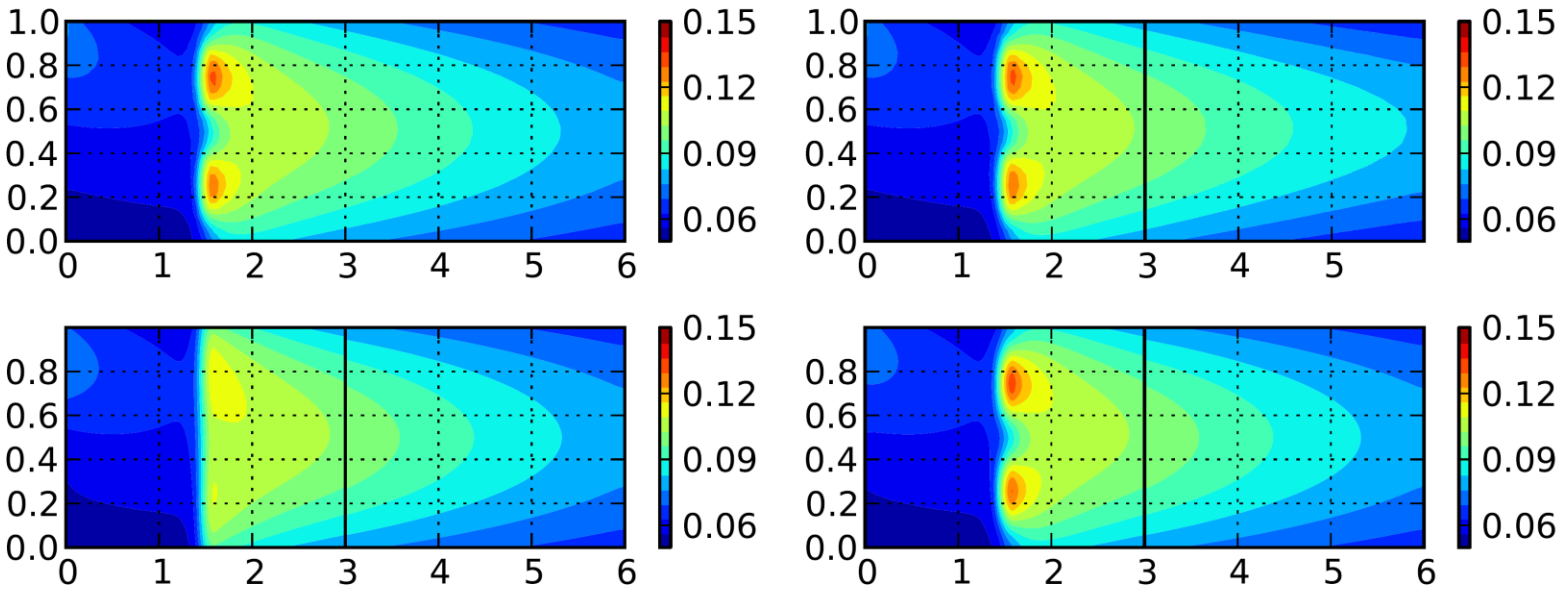

Figure 3: Full solution (top-left); geometrical multiscale solution (top-right) and Hi-Mod solution with $\{3, 1\}$ (bottom-left) and $\{5, 1\}$ (right) modes

HiMod more suitable for adaptive strategies